

MESTRADO
TOXICOLOGIA ANALÍTICA CLÍNICA E FORENSE

Evaluation of the phototoxicity of topical phenolic antioxidants.

Brandon Lage Aguiar

M
2018



Evaluation of the phototoxicity of
topical phenolic antioxidants

Brandon Lage Aguiar



Evaluation of the phototoxicity of topical phenolic antioxidants

Brandon Lage Aguiar

Dissertation of the 2nd Cycle of Studies Conducting of the Master's
Degree in Toxicologia Analítica Clínica e Forense

Supervisores: Prof. Doutora Isabel Almeida

Laboratório de Tecnologia Farmacêutica

Prof. Doutora Helena Carmo

Laboratório de Toxicologia

September of 2018

It is allowed the complete reproduction of this dissertation only for research purposes through a written declaration of the person concerned that such pledge.

Abstract

The skin is the largest organ of the body and the main barrier between the environment and the internal organs. Therefore, it is exposed to solar irradiation that may induce deleterious effects which can be increased by photosensitizer compounds. Through a phenomenon known as photosensitivity, these compounds, with the ability to absorb radiation in the 290-700 nm range, can suffer chemical reactions leading to undesirable effects in the skin.

Several *in vitro* methods have been developed to assess phototoxicity including the 3T3 Neutral Red Uptake Phototoxicity Test (3T3 NRU-PT) which is conducted with mouse fibroblasts (Balb/c 3T3 cells). However, when a compound is applied on the skin, it is firstly exposed to keratinocytes and therefore, testing phototoxicity in a human keratinocyte cell line might be more representative of the human *in vivo* situation when compared to the Balb/c 3T3 cell line.

The aim of this study was to evaluate the phototoxic potential of the *Castanea Sativa* leaf extract and some of its constituents alongside with a series of raw materials for use in cosmetic products. For this purpose, a previously implemented phototoxicity assay, in a human keratinocyte cell line (HaCaT) based on the 3T3 NRU-PT assay reported in the OCDE₄₃₂ guideline, using a UVA/UVB Osram lamp, was used. Additionally, a preliminary *in vitro* assay to determine the generation of Reactive Oxygen Species (ROS) was conducted to determine the photoreactivity of each compound.

The first step before conducting a phototoxicity assay is to determine if the compound absorbs UV/VIS light in the range of 290 -700 nm. Therefore, the absorption spectrum of all compounds was obtained, and all revealed strong absorbance within this wavelength range (with a molar extinction coefficient superior to 1000 L mol⁻¹ cm⁻¹), thus indicating possible phototoxicity.

Using quinine as a positive control, the ROS assay was implemented, and the feasibility study was conducted using some reference chemicals (benzocaine and erythromycin as negative reference chemicals and diclofenac and chlorpromazine hydrochloride (CPZ) as positive reference chemicals). This assay demonstrated that *Castanea sativa* leaf extract and 3,4-dihydroxyphenylacetic acid (DOPAC) were photoreactive while all other compounds were not photoreactive.

In the *in vitro* phototoxicity assay, the PIF values obtained for CPZ, quinine and *C. sativa* leaf extract were 17.89 ± 1.37 , 1.11 ± 0.01 and 12.00 ± 1.04 respectively. In the case of the phenolic antioxidants tested, the PIF values could not be calculated due to the lack

of toxicity preventing the determination of the IC₅₀ values necessary to calculate the PIF. Therefore, all test substances were found to be not phototoxic except for the *C. sativa* extract, and CPZ which was a positive control.

With this study we were able to conclude that *C. sativa* leaf extract is photoreactive and phototoxic. Since all the tested phenolic constituents of the extract were not phototoxic when tested individually, the compound(s) responsible for the phototoxicity of the extract remain unknown and further studies are necessary to fully understand the causes of its phototoxicity.

Key Words: Phototoxicity; Phenolic Antioxidants; Keratinocytes; Reactive Oxygen Species.

Resumo

A pele é o maior órgão do corpo humano e é a principal barreira entre o ambiente circundante e os órgãos internos. Por isso, a pele está exposta a radiação solar que pode induzir danos, que podem aumentar quando a exposição solar é combinada com compostos fotosensibilizadores. Através de um fenómeno conhecido como fotossensibilização, estes compostos que apresentam a capacidade de absorver radiação entre os 290-700 nm podem sofrer reações químicas originando efeitos indesejados na pele.

Vários métodos *in vitro* têm sido desenvolvidos para a avaliação da fototoxicidade, incluindo o ensaio 3T3 NRU-PT que é realizado em fibroblastos de rato (células Balb/c 3T3). No entanto, quando um composto é aplicado na pele, primeiramente entra em contacto com os queratinócitos e por este motivo, testes de fototoxicidade utilizando linhas celulares de queratinócitos humanos (HaCaT) podem ser mais representativos da situação *in vivo* em humanos quando comparados com a linha celular Balb/c 3T3.

O objetivo deste estudo foi avaliar o potencial fototóxico do extrato da folha da *Castanea sativa*, assim como alguns dos seus constituintes e também de uma série de matérias primas para uso cosmético. Para tal foi utilizado, um ensaio de fototoxicidade previamente implementado numa linha celular de queratinócitos humanos (HaCaT) baseado no ensaio 3T3 NRU-PT com uma lâmpada UVA/UVB (Osram) relatado na norma OCDE₄₃₂. Foi também realizado um ensaio preliminar para determinação da geração de espécies reativas de oxigénio (ROS) para determinar a fotoreatividade de cada composto.

O primeiro passo antes de realizar um ensaio de fototoxicidade é determinar se o composto absorve luz UV/VIS na gama de comprimento de onda compreendido entre 290-700 nm. Para tal, o espectro de absorção de todos os compostos nesta gama de comprimentos de onda foi obtido, revelando uma alta absorvência (com coeficientes de absorvidade molar superiores a $1000 \text{ L mol}^{-1} \text{ cm}^{-1}$), indicando assim possível fototoxicidade.

Utilizando a quinina como controlo positivo, o método de geração de ROS foi implementado e o estudo da fiabilidade do ensaio foi realizado usando alguns compostos de referência (benzocaína e eritromicina como compostos de referência negativos e diclofenac e cloridrato de chlorpromazina (CPZ) como compostos de referência positivos). Este ensaio revelou que o extrato da folha da *Castanea sativa* e o DOPAC são fotoreativos enquanto que todos os outros compostos não são fotoreativos.

No ensaio de fototoxicidade *in vitro*, os valores de PIF obtidos para a CPZ, quinina e o extrato da folha da *C. sativa* foram de 17.89 ± 1.37 , 1.11 ± 0.01 e 12.00 ± 1.04 respetivamente. No caso dos antioxidantes fenólicos, os valores de PIF não puderam ser calculados uma vez que não apresentaram toxicidade impedindo a determinação dos valores de IC50 e consequentemente do cálculo do PIF. Sendo assim, todos os compostos revelaram não ter potencial fototóxico exceto o extrato da folha da *C. sativa*, e a CPZ que é um controlo positivo.

Com este estudo concluímos que o extrato da *C. sativa* é fotoreativo e fototóxico. Uma vez que todos os compostos fenólicos testados identificados no extrato não são fototóxicos, quando testados individualmente, o(s) composto(s) responsável(veis) permanecem desconhecidos e serão necessários no futuro mais estudos para esclarecer as causas envolvidas na fototoxicidade do extrato.

Palavras Chave: Fototoxicidade; Antioxidantes fenólicos; Queratinócitos; Espécies Reativas de Oxigénio.

Abbreviations

3T3 NRU PT: 3T3 Neutral Red Uptake phototoxicity test

DNA: Deoxyribonucleic acid

ERO1: Endoplasmatic Reticulum Oxidoreductin-1

ETOH: Ethanol

FAD: Flavin Adenine Dinucleotide

ICH: International Conference on Harmonization

NADPH: Nicotine Adenine Dinucleotide Phosphate

NBT: Nitro blue tetrazolium

PDI: Protein Disulfide Isomerasese

PIF: Photo Irratation Factor

RNO: N,N-Dimethyl-4-nitrosoaniline

RNS: Reactive Nitrogen Species

ROS: Reactive Oxygen Species

UV: Ultraviolet

XO: Xanthine Oxidase

Acknowledgments

The realization of this dissertation would not be possible without the contribute of many people. To these people I want to express my gratitude.

I first want to thank my supervisors, Prof. Dra. Isabel Almeida and Prof. Dra. Helena Carmo for motivating me, for all the patience to explain every doubt I had, never letting me give up, for all the knowledge and dedication provided and specially for all the advises that helped me grow in a professional and personal level.

To Prof. Dr. Jorge Garrido, for all the help and support given throughout this work and for all the clarifications that allowed me to complete this project.

To my friends and colleagues Rita Pereira, Cláudia Tomé, Tânia Martins, Eva Martins, Ricardo Gonçalves, Vera Silva, Bárbara Silva, Telma Soares, Jorge Soares, Maria Enea, Patrícia Moreira, Cátia Faria, Margarida Silva, Maria Coelho, Rita Guedes, Daniela Rodrigues, Sofia Oliveira, Mariana Mozart, Beatriz Santos and all the others who helped me to stay motivated, on the right path and never gave up on me and made this journey a lot easier.

To Dr. Renata Silva and Dr. Diana Silva for all the knowledge and time given, without it I would not have this work.

To all my family, in particular my parents and my brother for supporting me in every situation.

Index

Abstract	III
Resumo	V
Abbreviations	VII
Acknowledgments	VIII
Index	IX
Table Index	XI
Figure Index	XII
Equation Index	XIV
1. INTRODUCTION	1
1.1 Skin structure	1
1.1.1 Epidermis	1
1.1.2 Dermis	3
1.1.3 Hypodermis	3
1.2 Oxidative stress and Reactive Species	3
1.2.1 Skin oxidative stress	4
1.2.1.1 Endogenous sources of ROS on the skin	4
1.2.1.1.1 Mitochondrial ROS production	4
1.2.1.1.2 Peroxisome ROS production	5
1.2.1.1.3 Heavy metal ions	5
1.2.1.2 Exogenous sources of ROS	6
1.2.1.2.1 Solar Irradiation	6
1.2.1.2.2 Cigarette smoke	6
1.2.1.2.3 Ionizing Radiation	7
1.3 Antioxidants	7
1.3.1 Endogenous antioxidants	7
1.3.2 Exogenous antioxidants	8
1.4 Photosensitivity	8
1.4.1 Phototoxicity	9
1.4.2 Photochemical reaction	10
1.5 Phototoxicity evaluation	12
1.5.1 Factors to consider in the phototoxicity evaluation	13
1.5.2 <i>In vitro</i> phototoxicity evaluation	13
1.5.3 ROS generation assay	16
1.6 Phenolic antioxidants analyzed	17
2. AIM	21

3. MATERIALS AND METHODS	22
3.1 Materials	22
3.1.1 Raw materials	22
3.1.2 Laboratory materials	22
3.2 Methods	22
3.2.1 Cell culture	22
3.2.1.1 HaCaT cell line	23
3.2.1.2 Phototoxicity Study	23
3.2.2 <i>Castanea Sativa</i> leaf extract preparation	25
3.2.3 Spectral Absorption	25
3.2.4 ROS generation Assay	26
3.2.4.1 Optimization of the ROS assay	26
3.2.4.2 ROS Assay	26
4. RESULTS AND DISCUSSION	27
4.1 Spectral Absorption	27
4.2 ROS generation assay	31
4.3 Neutral red uptake phototoxicity assay	33
4.3.1 HaCaT cell line characterization	33
4.3.2 Solvent control	34
4.3.3 Positive controls	35
4.3.3.1 Chlorpromazine	35
4.3.3.2 Quinine	36
4.3.4 Raw Materials	37
4.3.4.1 Caffeic acid	37
4.3.4.2 Ferulic acid	38
4.3.4.3 p-Coumaric acid	39
4.3.4.4 3,4-dihydroxyphenylacetic acid (DOPAC)	40
4.3.4.5 <i>Castanea sativa</i> leaf extract	40
4.3.4.6 Chlorogenic acid	41
4.3.4.7 Ellagic acid	42
4.3.4.8 Rutin	43
5. CONCLUSIONS	46
6. REFERENCES	48

Table Index

Table 1. List of oxygen and nitrogen reactive species generated in the skin. Adapted from (13).	4
Table 2. Antioxidant enzymes and non-enzymatic antioxidants. Adapted from (32).	8
Table 3. Exogenous antioxidants. Adapted from (33).	8
Table 4. Photobiological reactions of chemicals in the presence of UV/VIS light. Adapted from (34).	9
Table 5. Phototoxicity testing methods in vitro. Adapted from (51).	15
Table 6: Information of the phenolic antioxidants analyzed.	18
Table 7: Summary of tested compounds, solvents used, and concentrations tested. ..	24
Table 8: Molar absorptivity and maximum wavelength of the tested compounds at 10 µg/mL.	30
Table 9: Summary of the results obtained for each compound using the ROS generation assay.	32
Table 10: Summary of data obtained with the phototoxicity and ROS generation assays.	45

Figure Index

Figure 1: Skin structure. Adapted from (5).	1
Figure 2: Epidermis layers. Reproduced from (7).	2
Figure 3: Reduction of molecular oxygen into water and hydrogen peroxide. Reproduced from (18).	5
Figure 4: Phototoxicity initiated with UV light. Reproduced from (24).	9
Figure 5: Different types of UV radiation and their penetration into the skin. Reproduced from (40).	10
Figure 6: Chemical structure of chlorpromazine. Adapted from (41).	11
Figure 7: Basic processes in photochemistry. The ground state molecule absorbs a photon (step a); the excited singlet state returns to the ground state by releasing heat or light (step b); or undergoes a chemical reaction (step c); or converts to an excited triplet state by intersystem crossing (step d); the excited triplet state releases heat or light (step e); or transfers energy to an molecular oxygen forming singlet oxygen (step f); or transfers an electron generating a radical (step g); This radical can form an adduct by covalent binding with a biomolecule (step h) or generate an oxygen radical if molecular oxygen is the electron acceptor. Adapted from (43, 44).	12
Figure 8: Initial evaluation of phototoxicity. Adapted from (46).	13
Figure 9: Photo-Irritation-Factor (PIF) to determine the phototoxic potential of a compound. Adapted from (24).	15
Figure 10. A) 3,4-dihydroxybenzoic acid spectral absorption and B) 3,4-dihydroxyhydrocinnamic acid spectral absorption.	27
Figure 11. A) 3,4-dihydroxyphenylacetic acid spectral absorption and B) Caffeic acid spectral absorption.	27
Figure 12. A) C. sativa extract spectral absorption and B) Chlorogenic acid spectral absorption.	27
Figure 13: A) CPZ spectral absorption and B) Ellagic acid spectral absorption.	28
Figure 14. A) Ferulic acid spectral absorption and B) p-Coumaric acid spectral absorption.	28
Figure 15. A) Quercetin spectral absorption and B) Quinine spectral absorption.	28
Figure 16. Rutin spectral absorption.	28
Figure 17: Photoreactivity criteria for the ROS assay. Adapted from (52).	32
Figure 18: Determination of HaCat cell line doubling time by linear regression analysis.	34

Figure 19: Cell viability of HaCaT cell line exposed to solvent by the Neutral Red assay. Data are presented as mean \pm SD (n=3). Data were analyzed using One-way ANOVA with Dunnett post hoc test.....	35
Figure 20: Cell viability of HaCaT cell line exposed to solvent control by the Neutral Red assay after irradiation. Data are presented as mean \pm SD (n=3). Data were analyzed using One-way ANOVA with Dunnett post hoc test. **** p< 0.0001 vs. Cells *** p< 0.001.	35
Figure 21: Cell viability of HaCaT cell line exposed to chlorpromazine, determining the phototoxicity by the Neutral Red assay. Irr-: Non-irradiated. Irr+: Irradiated plate. Data are presented as mean \pm SD (n=3) relative to solvent control.	36
Figure 22: Cell viability of HaCaT cell line exposed to quinine, determining the phototoxicity by the Neutral Red assay. Irr-: Non-irradiated. Irr+: Irradiated plate. Data are presented as mean \pm SD (n=3) relative to solvent control.	37
Figure 23: Cell viability of HaCaT cell line exposed to caffeic acid, determining the phototoxicity by the Neutral Red assay. Irr-: Non-irradiated. Irr+: Irradiated plate. Data are presented as mean \pm SD (n=3) relative to solvent control.	38
Figure 24: Cell viability of HaCaT cell line exposed to ferulic acid, determining the phototoxicity by the Neutral Red assay. Irr-: Non-irradiated. Irr+: Irradiated plate. Data are presented as mean \pm SD (n=3) relative to solvent control.	39
Figure 25: Cell viability of HaCaT cell line exposed to p-coumaric acid, determining the phototoxicity by the Neutral Red assay. Irr-: Non-irradiated. Irr+: Irradiated plate. Data are presented as mean \pm SD (n=3) relative to solvent control.	39
Figure 26: Cell viability of HaCaT cell line exposed to 3,4-dihydroxyphenylacetic acid, determining the phototoxicity by the Neutral Red assay. Irr-: Non-irradiated. Irr+: Irradiated plate. Data are presented as mean \pm SD (n=3) relative to solvent control. ..	40
Figure 27: Cell viability of HaCaT cell line exposed to Castanea sativa extract, determining the phototoxicity by the Neutral Red assay. Irr-: Non-irradiated. Irr+: Irradiated plate. Data are presented as mean \pm SD (n=3) relative to solvent control. ..	41
Figure 28 Cell viability of HaCaT cell line exposed to chlorogenic acid, determining the phototoxicity by the Neutral Red assay. Irr-: Non-irradiated. Irr+: Irradiated plate. Data are presented as mean \pm SD (n=3) relative to solvent control.	42
Figure 29: Cell viability of HaCaT cell line exposed to ellagic acid, determining the phototoxicity by the Neutral Red assay. Irr-: Non-irradiated. Irr+: Irradiated plate. Data are presented as mean \pm SD (n=3) relative to solvent control.	43
Figure 30: Cell viability of HaCaT cell line exposed to rutin, determining the phototoxicity by the Neutral Red assay. Irr-: Non-irradiated. Irr+: Irradiated plate. Data are presented as mean \pm SD (n=3) relative to solvent control.....	44

Equation Index

Equation 1: Production of superoxide anion mediated by NADPH. Reproduced from (19).	5
Equation 2: Haber-Weiss. Reproduced from (28).....	6
Equation 3: Fenton reaction. Reproduced from (28).	6
Equation 4. Chemical reaction leading to the bleaching of RNO.	16
Equation 5. Reduction of NBT to NBT ⁺	16
Equation 6. Cell viability (%).	25
Equation 7: Photo Irritation Factor (PIF).....	25
Equation 8. Beer-lambert equation where A= Absorbance, ϵ = Molar extinction coefficient (L mol ⁻¹ cm ⁻¹); c= concentration (L mol ⁻¹); l=Length (cm)	29
Equation 9. Equation of the decreased absorbance of RNO by singlet oxygen. Reproduced from (52).....	31
Equation 10. Equation of the increased absorbance of NBT due to the formation of NBT ⁺ . Reproduced from (52).....	31

1. INTRODUCTION

1.1 Skin structure

Among all the organs in our body, the skin is the largest, acting as a barrier against several external agents (1, 2) with functions ranging from sensory protection, excretion and absorption, to thermoregulation, fluid balance and physical, chemical and biological protection (1, 3).

As can be depicted in **Figure 1**, the skin is divided into layers with different functions. The epidermis is the most external layer and contacts directly with the external environment. The dermis is formed below, (2) followed by the deeper layers of subcutaneous tissue, the hypodermis, that consist of fat and connective tissue (4).

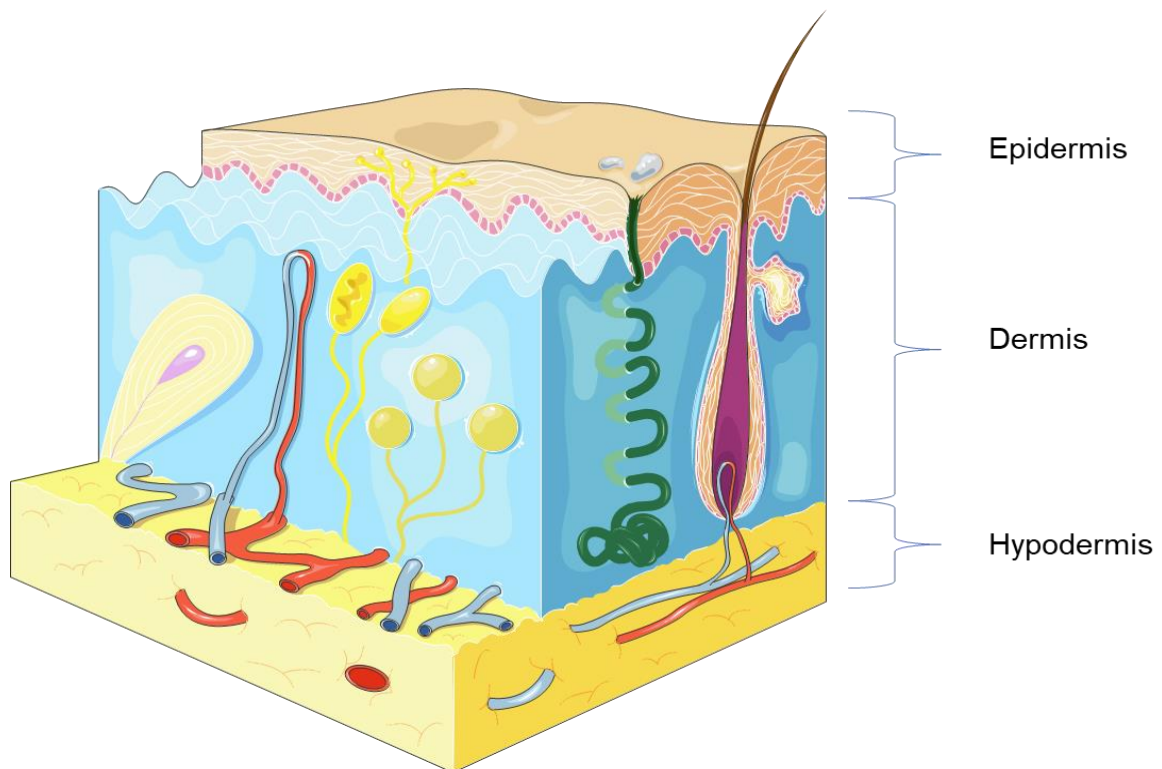


Figure 1: Skin structure. Adapted from (5).

1.1.1 Epidermis

The epidermis is the outermost layer of the skin, being in direct contact with the environment and working as a barrier, protecting the skin from potentially hazardous environmental threats. It is subdivided into different layers depicted in **Figure 2**. The deepest layer, the basal layer, which is just above the dermis is followed by the spinous and granular layers and finally by the *stratum corneum*, the first barrier of the skin (6).

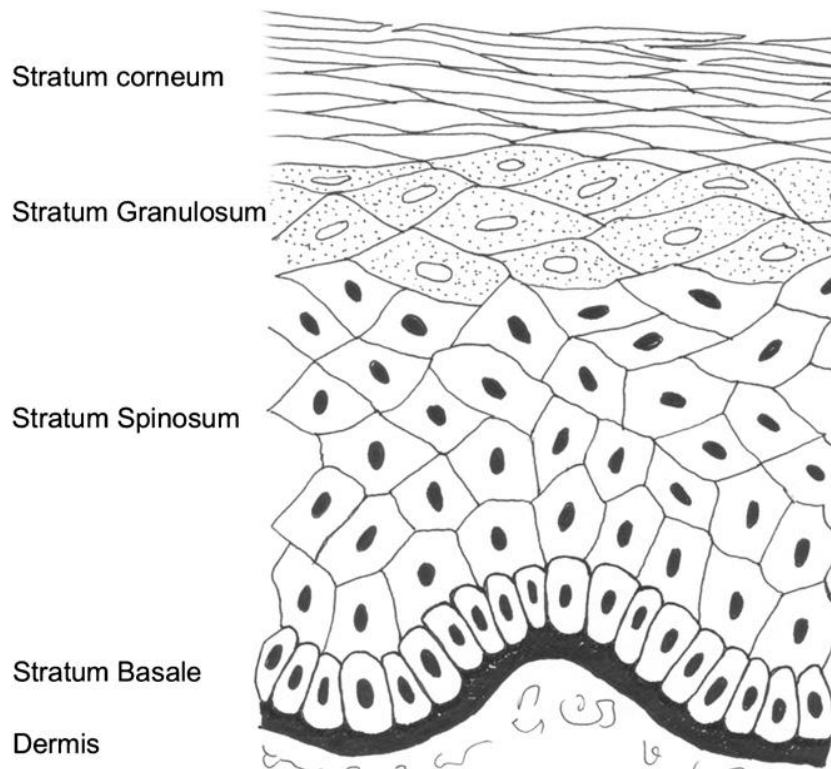


Figure 2: Epidermis layers. Reproduced from (7).

The epidermis has four main types of cells: keratinocytes, melanocytes, langerhans cells and merkel cells. Among all these, the keratinocytes are the most abundant type of cells that exist in the epidermis and are responsible for the synthesis of various structural proteins and lipids (1). Keratinocytes produce keratins which are the most important skin structural proteins. They are present from the basal to the granular layer and after that point they are called corneocytes (7).

Melanocytes are found in the basal layer. They are responsible for the protection against ultraviolet radiation (UV) and for this purpose, they produce pigmented granules called melanosomes that contain melanin (6, 7). Melanogenesis is the physiological process that leads to the biosynthesis of melanin (8). This process is continuous and is accelerated by UV exposure resulting in the phenomenon commonly referred to as “tanning” which generally appears 2-3 days after sunburn and due to the epidermal turnover, disappears within a month (7, 9). Melanin is very important for UV protection since it can absorb up to 75% of UV radiation that reaches the skin (4).

The langerhans cells are dendritic cells that are very important for the immune barrier and participate mainly in allergic contact events (6).

The merkel cells can mostly be found in the basal layer of the epidermis and are sensorial receptors when associated with nerve terminals. They can also be part of the neuroendocrine system (10).

1.1.2 Dermis

The dermis is a connective tissue that supports and compacts the skin. It is highly vascularized and has a large network of lymphatic vessels. The main cells that compose the dermis are fibroblasts and macrophages (6). The fibroblasts synthesize and renew the extracellular matrix and the macrophages eliminate foreign material and damaged tissue (6).

1.1.3 Hypodermis

The deepest layer of the skin is the hypodermis, a subcutaneous fat compartment that is well supplied with blood vessels and nerves. It affords protection against mechanical shocks, isolates the body from the external temperature, and ensures general energy metabolism and storage (6, 11).

1.2 Oxidative stress and Reactive Species

The presence of reactive species leads to adverse effects on the human body such as DNA damage, cell cycle dysregulation and DNA repair/or replication disturbance. Since the skin is the first barrier against external insults, it becomes a major target for oxidative stress. The generation of reactive species does not arise only from endogenous sources but also from exogenous sources such as pollution, atmospheric gases, UV radiation, microorganisms, viruses and xenobiotics (2).

Reactive Oxygen Species (ROS) are among the most important agents that induce damage to the cells (12). Despite their negative effects, at low concentrations, ROS have important roles in cell signaling, cell growth, smooth muscle relaxation, immune responses, synthesis of biological molecules, homeostasis and blood pressure modulation (13) (14). When the balance between the concentration of ROS and the level of antioxidants falls in favor of ROS concentration then the phenomenon of oxidative stress occurs (15). Oxidative stress leads to a variety of pathological conditions such as cancer, neurological disorders, atherosclerosis, hypertension, pulmonary disease and more (16). Similar effects occur when Nitrogen Reactive Species (RNS) are involved (15).

ROS/RNS can be divided into two groups: (i) molecules that contain one or more unpaired electrons which confer a high reactivity to the molecule are called free radicals,

and (ii) when 2 free radicals share their unpaired electrons this molecule is called a nonradical (16).

Some of the most important radical and non-radical species are presented in **Table 1**.

Table 1: List of oxygen and nitrogen reactive species generated in the skin. Adapted from (13).

Radical Species		Non-radical species	
Superoxide anion	$O_2^{\bullet -}$	Hydrogen peroxide	H_2O_2
Hydroxyl	HO^{\bullet}	Singlet Oxygen	$O_2^1\Delta_g$
Peroxyl radical	ROO^{\bullet}	Peroxynitrite	$ONOO^-$
Radical hydroperoxide	HOO^{\bullet}	Nitrite	NO_2^-
Nitric oxide	$N^{\bullet}O$	Nitrate	NO_3^-

1.2.1 Skin oxidative stress

The health and appearance of the skin is a reflection of many factors such as genetics, environmental factors, nutrition and habits like smoking and alcohol abuse. Oxidative stress is the main source of damage to the skin cells (4).

1.2.1.1 Endogenous sources of ROS on the skin

As a result of normal cellular metabolism, ROS can be produced from molecular oxygen (16). There are several intracellular sources for the production of ROS, and the most relevant are listed below.

1.2.1.1.1 Mitochondrial ROS production

Since our organism is under aerobic conditions, even though most of the oxygen consumed is reduced to water, a small percentage of the molecular oxygen is reduced to the superoxide anion ($O_2^{\bullet -}$) which is quickly converted into H_2O_2 . Although it is not a free radical, H_2O_2 is highly reactive. H_2O_2 can split up into HO^{\bullet} which is a highly reactive free radical, by accepting one electron (**Figure 3**) (17).

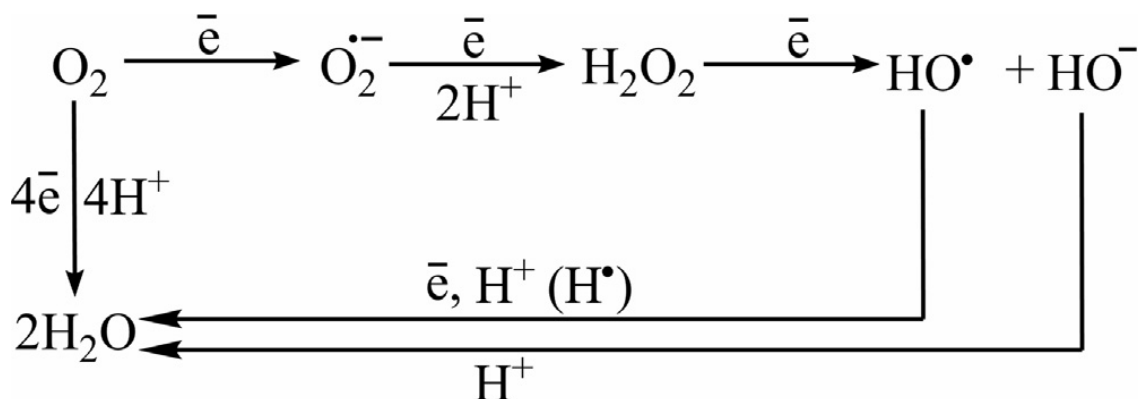


Figure 3: Reduction of molecular oxygen into water and hydrogen peroxide. Reproduced from (18).

Superoxide anion ($\text{O}_2^{\bullet -}$) is produced when one electron is added to molecular oxygen. This process can be mediated by Nicotine Adenine Dinucleotide Phosphate (NADPH) oxidase or Xanthine Oxidase (XO) or by the mitochondrial electron transport system. (16)

A sudden and rapid electron transfer from NADPH to the molecular oxygen generates $\text{O}_2^{\bullet -}$ as represented in **Equation 1**(19).

Equation 1: Production of superoxide anion mediated by NADPH. Reproduced from (19).



Inside the mitochondrial membrane occurs the electron transport chain. At the end, an electron reduces molecular oxygen to produce H_2O . However, electrons can leak prematurely to O_2 and form $\text{O}_2^{\bullet -}$ instead of water (12). In the skin, 1.5-5% of the oxygen consumed is converted into ROS mainly within the mitochondria of keratinocytes and fibroblasts (20).

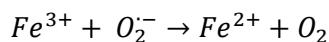
1.2.1.1.2 Peroxisome ROS production

Peroxisomes are filled with a wide range of enzymes, mainly flavoenzymes/oxidoreductases that can produce not only H_2O_2 as a byproduct but also $\text{O}_2^{\bullet -}$ mainly with the contribution of the enzyme XO (12). This enzyme's activity involves the reduction of molecular oxygen, resulting in the formation of $\text{O}_2^{\bullet -}$ (21).

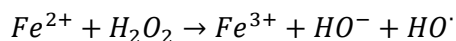
1.2.1.1.3 Heavy metal ions

Transition metals like copper, iron, and nickel can interact with $\text{O}_2^{\bullet -}$ and H_2O_2 via the metal catalyzed Haber-Weiss/Fenton, represented in **Equation 2** and **Equation 3** and induce generation of hydroxyl radicals and consequently lead to cellular damage through lipid peroxidation and reacting with nuclear proteins and DNA that leads to the depletion of enzymes activities of superoxide dismutase, catalase, glutathione and glutathione peroxidase (16, 22).

Equation 2: Haber-Weiss. Reproduced from (22).



Equation 3: Fenton reaction. Reproduced from (22).



1.2.1.2 Exogenous sources of ROS

1.2.1.2.1 Solar Irradiation

The most damaging solar radiation is the UV radiation. Although this radiation offers some benefits to the human health and increases the vitamin D levels it's also the major exogenous factor that damages the skin (8, 23). The sunlight that reaches the earth is composed by 6/7% of UV light, 42% of visible light and 51% of infrared radiation. These different types of radiation have different wavelengths and different levels of energy, being the UV the most energetic of the three and with the shortest wavelength (24). The UV light can be divided into UVA (320-400 nm), UVB (280-320 nm) and UVC (200-280 nm). The UVC radiation despite being mutagen, is absorbed by the stratospheric ozone layer causing little damage to the skin. On the other hand, 95% of the UV radiation that reaches the earth is UVA and the remaining 5% is UVB (25).

For the UVB radiation, the damage happens on the epidermis through direct damage on DNA and in cases of long-term exposure it can cause sunburn and skin cancer. On the other hand, UVA radiation can reach deep dermal layers and generate ROS which not only damage the DNA but also the collagenous extracellular matrix of connective tissues, disrupt dermis integrity, and play crucial roles in photoaging, skin cancer and induction of sun tanning and pigmented spots (18).

Several studies have suggested that sunscreens incorporated with antioxidants with the ability to diminish the sun-induced ROS formation have more benefits for the skin, demonstrating the importance of controlling the formation of ROS in order to minimize skin damage (18).

1.2.1.2.2 Cigarette smoke

Cigarette smoke is composed of many oxidants and reactive species such as superoxide and nitric oxide, which will increase the concentration of ROS in the organism. Also, inhaling cigarette smoke into the lungs leads to the activation of endogenous mechanisms such as the accumulation of neutrophils and macrophages which will further increase the oxidant injury since they are inflammatory cells and release ROS (16, 26). Smoking has been shown to be a risk factor in the development of wrinkles on the skin. The

negative effects of smoking on the skin may be due to different mechanisms. A decrease in the stratum corneum moisture of the face is probably caused by the direct toxicity of the smoke causing wrinkles and the so-called facial smoker's wrinkles, but the dermis may also be affected indirectly by the toxic compounds of the smoke via the blood stream (27).

1.2.1.2.3 Ionizing Radiation

Ionizing radiation has enough energy to induce a homolytic fission of one of the O-H bonds from H_2O_2 generating hydroxyl radical that accounts for much of the damage inflicted by ionizing radiation to living beings (28).

1.3 Antioxidants

Since the skin is in contact with environmental factors that lead to oxidative stress such as UV radiation, to protect itself it uses defense mechanisms such as antioxidants (29). Antioxidants have the ability to scavenge or neutralize reactive species formation and prevent, delay, or remove oxidative damage inflicted by these reactive species (30). As mentioned before regarding the efficacy of sunscreens, it has been suggested that an increased intake of antioxidants by topical application may be successful in enriching the endogenous cutaneous system preventing oxidative damage to the cells (8, 31).

Antioxidants can be divided into two major groups: endogenous antioxidants (produced by the organism) and exogenous antioxidants (obtained by diet or external application) (4).

1.3.1 Endogenous antioxidants

In order to protect themselves from ROS, the cells are equipped with endogenous antioxidants that help keeping the balance between ROS formation and elimination, to maintain homeostasis and avoid the generation of oxidative stress and accompanying negative effects (30).

For the endogenous defense system of the skin, there are two crucial groups of antioxidants: antioxidant enzymes and non-enzymatic molecules, being the most important ones represented in **Table 2** (32).

Table 2: Antioxidant enzymes and non-enzymatic antioxidants. Adapted from (32).

Antioxidant enzymes	Non-enzymatic antioxidants
Peroxide dismutase	Ascorbic Acid
Catalase	Glutathione
Glutathione peroxide	Uric acid
Thioredoxin Reductases	Tocopherols
NADPH quinone reductase	Coenzyme Q
Heme oxygenase	β-carotene
	Melanin

1.3.2 Exogenous antioxidants

The endogenous defense system is frequently insufficient to protect the cells from all the sources of ROS that the skin is exposed to, and it has been demonstrated that these antioxidants defenses decline with age. Therefore, in order to balance the concentration of ROS with the concentration of antioxidants it is recommended that the amount of antioxidants is increased through diet or topical application (4).

Some examples of exogenous antioxidants are shown in **Table 3**.

Table 3: Exogenous antioxidants. Adapted from (33).

Vitamins (C and E)
Trace elements (zinc and selenium)
Carotenoids
Phenolic acids (caffeic acid, chlorogenic acid, gallic acid...)
Flavanols
Anthocyanidins
Isoflavones
Flavanones
Flavones

1.4 Photosensitivity

Photosensitivity consists in an abnormal reaction to sunlight that includes phototoxicity, photoallergy, photogenotoxicity, and photocarcinogenicity, which are summarized in **Table 4** (9).

Table 4: Photobiological reactions of chemicals in the presence of UV/VIS light. Adapted from (34).

Phototoxicity	Acute reaction similar to a sunburn that can occur after a single exposure to a photochemical
Photoallergy	An immunological reaction that occurs after multiple exposures to a photochemical
Photogenotoxicity	The capacity of a compound to be activated by UV/VIS radiation into a genotoxin.
Photocarcinogenicity	The capacity of a compound to be activated by UV/VIS radiation into a carcinogen.

1.4.1 Phototoxicity

Phototoxicity is the most common type of photosensitive reaction and occurs when a photoactive or as sometimes called photoreactive chemical that is in contact or absorbed by the skin, is exposed to sunlight, is photoactivated leading to photoreactivity through the products of this reaction that are cytotoxic to the skin tissue, as represented in **Figure 4** (24). Since it is an acute response of the skin induced by sunlight to photoreactive chemicals, most of the clinical manifestations resemble skin irritation (24).

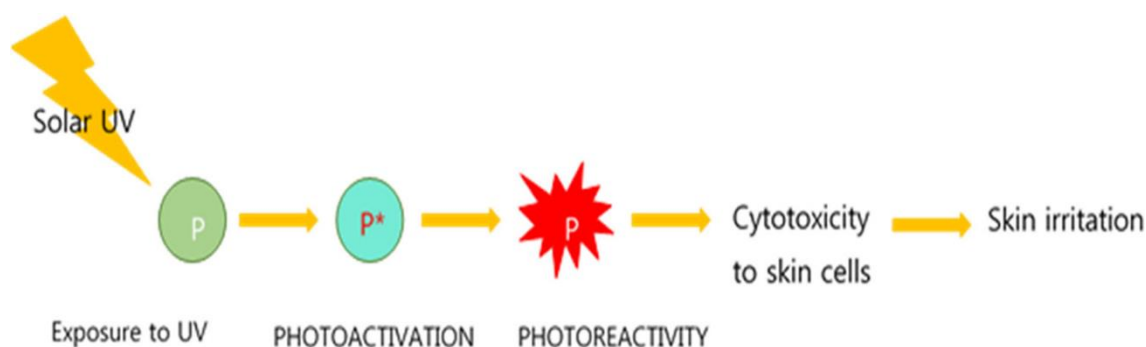


Figure 4: Phototoxicity initiated with UV light. Reproduced from (24).

Because the skin is continuously exposed to sunlight irradiation it is the organ most affected by phototoxicity (24).

Due to the fact that the levels of UV radiation reaching the Earth have been increasing due to the depletion of the protective ozone layer and, although chemical-induced phototoxicity in most cases might not be life-threatening, it can have a negative impact in the quality of life. For these reasons, the concern with phototoxicity has become greater (35-37).

For a phototoxic reaction to take place it is required an exposure to UV/VIS light in the range of 290 -700 nm but especially [UVA (320-400 nm) and UVB (290-320nm) and the

presence of the photoreactive chemical in the skin (38). Since the UVB has the shortest wavelength and consequently has more energy it inflicts severe damage to the DNA, although, as we can see in **Figure 5** it has a poor skin penetration and can only reach the epidermis. On the other hand, the UVA goes through the earth's atmosphere without being absorbed and can penetrate deeper into the subcutaneous layer making it the main responsible for phototoxic reactions since it can interact with drugs and chemicals distributed in deeper levels of the cutaneous tissue (20, 24, 39).

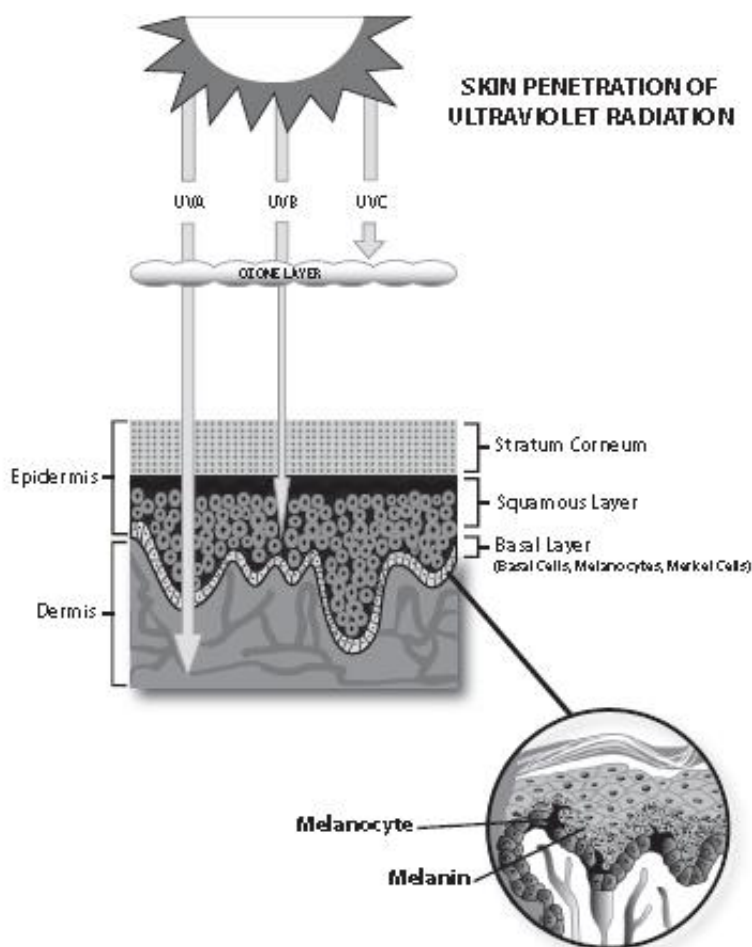


Figure 5: Different types of UV radiation and their penetration into the skin. Reproduced from (40).

1.4.2 Photochemical reaction

Since it is necessary that photochemicals absorb UV/VIS irradiation, any chemical that does not absorb in this range of the spectrum cannot cause phototoxicity. For a molecule to absorb in this range of the spectrum, it has to have chromophores such as double bonds and/or aromatic rings, for example chlorpromazine, that is a known photochemical represented in **Figure 6** (24).

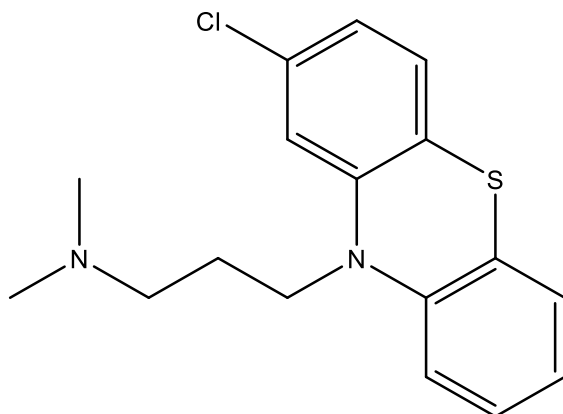


Figure 6: Chemical structure of chlorpromazine. Adapted from (41).

Mechanisms of phototoxicity can be divided into direct and indirect. In the direct mode the photoreactive chemical is excited after UV irradiation and reacts directly with the endogenous molecules whereas in the indirect mode the photoproducts (such as ROS) of the photoreactive chemical react with the endogenous molecules (24).

According to the second law of photochemistry, the Stark-Einstein law, only one molecule is activated for each photon of light absorbed (42). As we can see in **Figure 7**, when the molecule absorbs a photon of UV-Vis light, it goes from a ground state to an excited state. This excited state is very short-lived (in the order of nanoseconds) and it's very unstable so the molecule quickly returns to the ground state by dissipating the energy as heat or light or goes through a chemical reaction (direct mechanism of phototoxicity). However, some molecules after light absorption, through intersystem crossing, effectively cross over to a long-lived triplet state (lifetime in the order of microseconds and milliseconds) which is enough for a molecule to gain the ability to transfer this excess energy or charge to another molecule like oxygen (indirect mechanism of phototoxicity) (20, 43, 44).

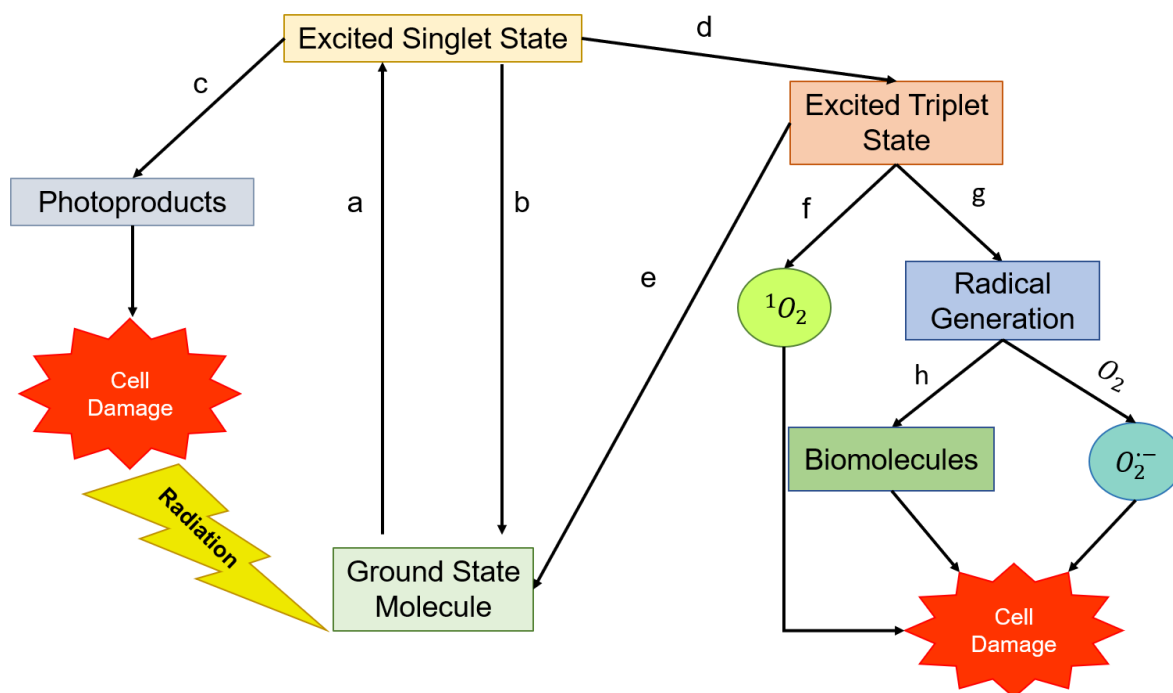


Figure 7: Basic processes in photochemistry. The ground state molecule absorbs a photon (step a); the excited singlet state returns to the ground state by releasing heat or light (step b); or undergoes a chemical reaction (step c); or converts to an excited triplet state by intersystem crossing (step d); the excited triplet state releases heat or light (step e); or transfers energy to an molecular oxygen forming singlet oxygen (step f); or transfers an electron generating a radical (step g); This radical can form an adduct by covalent binding with a biomolecule (step h) or generate an oxygen radical if molecular oxygen is the electron acceptor. Adapted from (43, 44).

As previously explained, although it is necessary the absorption of light to trigger a photochemical reaction, it does not mean that the absorption of light will inevitably lead to a phototoxic reaction since the dissipation of energy by heat, fluorescence or phosphorescence will not cause phototoxicity (42).

1.5 Phototoxicity evaluation

Evaluating the photo safety of a chemical is of high importance at an early stage of the drug discovery because it can prevent the appearance of undesirable drug reactions in humans and it is currently a regulatory requisite for all pharmaceuticals (34). Several types of drugs, such as antibiotics, anticonvulsants, antimalarials, antipsychotics, thiazide diuretics, non-steroidal anti-inflammatory drugs and others, have the potential to cause phototoxic reactions (45). Since cosmetics are often designed to be topically applied in order to prevent cosmetic phototoxicity, increased attention for photosafety assessment of cosmetic ingredients and products has arisen (35).

1.5.1 Factors to consider in the phototoxicity evaluation

In **Figure 8**, a flow chart describing the stepwise process of phototoxicity evaluation is represented.

Firstly, the chemical must absorb UV/VIS light in the range of 290 -700 nm. As explained previously if a compound does not absorb in this range there is no use of evaluating its phototoxicity (34).

Also, the test, compound must have the capability to be distributed to tissues that are exposed to light, more specifically the skin and the eyes, in order to be considered eligible for photosafety evaluation (46).

The production of ROS leads to cytotoxicity due to processes of oxidation of DNA, lipids and proteins, so if a chemical after being exposed to UV/VIS irradiation forms ROS, then it's advised to proceed to a photosafety evaluation (45, 46).

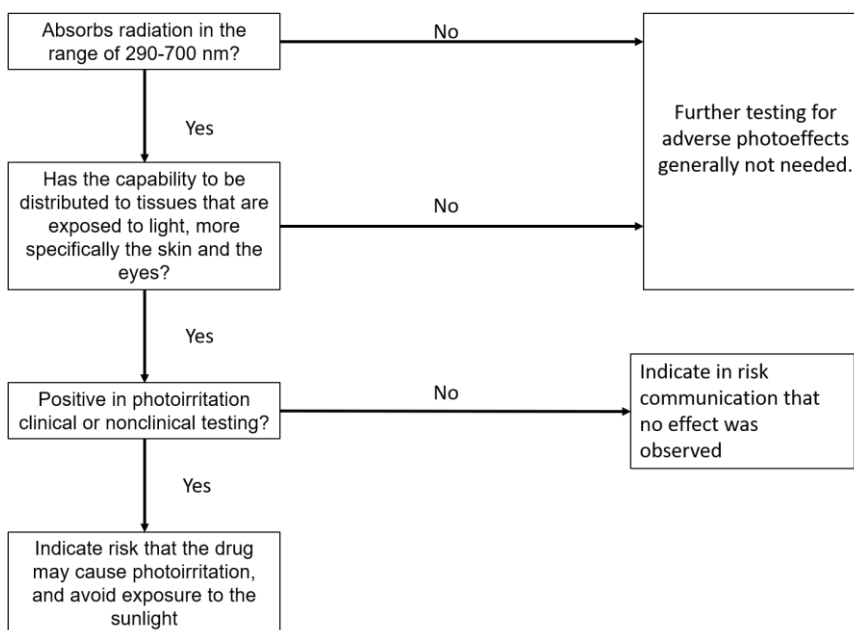


Figure 8: Initial evaluation of phototoxicity. Adapted from (46).

1.5.2 *In vitro* phototoxicity evaluation

Evaluating the photosafety is of special interest for cosmetics since they are products intended for application on the external surface of our body, namely the epidermis, therefore greatly exposed to sunlight radiation. This evaluation has been generally carried out by *in vivo* and *in vitro* tests. However, in order to protect the welfare of animals, *in vitro* testing has been used to replace the *in vivo* testing since these have been banned for

cosmetics (3, 35). To reach this objective, according to the ICH guidance S10 we should follow the 3R principles that stands for Replacement, Reduction and Refinement (47). Some of the recommended non-animal testing methods for phototoxicity are represented in **Table 5**.

The 3T3 NRU-PT (Neutral Red Uptake Phototoxicity Assay) is an *in vitro* method that can be used to determine the phototoxic potential of a compound and has been officially approved by OECD. For this purpose, this assay compares the cells viability when exposed to the test chemical, in presence or absence of UV/VIS irradiation, using vital dye, neutral red, which is a weak cationic dye that has the ability of penetrating cell membranes and accumulate only in viable cells. In this assay it is used the base cell-line Balb/c 3T3 cell, that corresponds to fibroblasts from mouse (24). However, some studies have shown that the 3T3 NRU PT appears to be oversensitive leading to various false-positive results when compared to *in vivo* photosafety tests (48, 49). False-positives can lead to several consequences such as: additional preclinical studies *in vivo* which will increase animal usage, additional cost and time developing new drugs and delaying the access of patients to new treatments and has implications on patient informed consent and product labeling documents (49). For this reason, the HaCaT cell line appears to be more representative of the human *in vivo* situation since it uses human keratinocytes which are the most abundant type of cells present in the external layer of the human skin, where the topical compounds would be applied and exposed to the sun radiation.

In order to predict the phototoxicity potential of a substance the Photo-Irritation-Factor (PIF) or Mean Photo Effect (MPE) should be determined. PIF is calculated by dividing the value obtained for the IC₅₀ (concentration where the cell viability is decreased by 50%) of the non-irradiated plate over the IC₅₀ of the irradiated plate as show in **Figure 9**. As represented in **Figure 9**, according to the OECD Test Guideline 432, a test chemical is considered phototoxic if a PIF value of 5 or superior is obtained. Values between 2 and 5 are considered as probable phototoxic and a PIF value inferior to 2 is considered non phototoxic (24, 50).

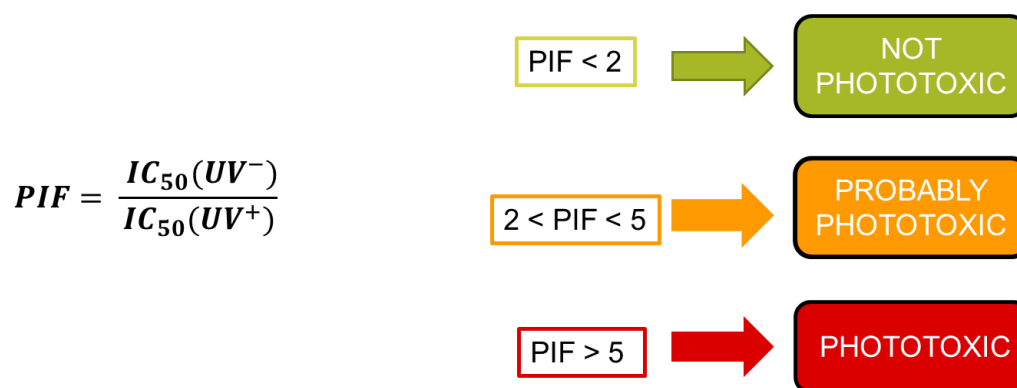


Figure 9: Photo-Irritation-Factor (PIF) to determine the phototoxic potential of a compound. Adapted from (24).

Table 5: Phototoxicity testing methods in vitro. Adapted from (51).

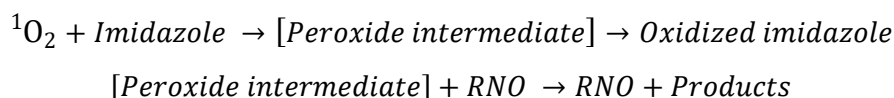
Tests	Cells	Determinations
3T3 NRU PT (50)	-Mice BALB/c 3T3 fibroblasts - Human keratinocyte cell line (HaCaT)	Phototoxicity Photo-Cytotoxicity
Reconstituted human skin models	Skin fibroblasts (dermal models) - Skin keratinocytes and a stratum corneum (epidermal models) - Fibroblasts, keratinocytes and a stratum corneum (full skin models)	Phototoxicity
Red Blood Cell Phototoxicity	- Mammalian erythrocytes	Phototoxicity (Photohaemolysis)
Yeast Assay	Facultative anaerobic yeast such as <i>S. cerevisiae</i>	Phototoxicity Photocytotoxic Photomutagenic Genotoxicity Photogenotoxicity

1.5.3 ROS generation assay

As previously mentioned, ROS in many phototoxic reactions are the main source of cytotoxicity. Therefore, a ROS generation assay has been proposed with the intention of detecting singlet oxygen ($^1\text{O}_2$) and superoxide anion ($\text{O}_2^{\bullet-}$) generated from photo-irradiated chemicals since these are the main ROS generated in a phototoxic reaction (36).

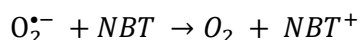
The $^1\text{O}_2$ generation can be detected by spectrophotometric measurement of N,N-Dimethyl-4-nitrosoaniline (RNO) bleaching followed by decreased absorbance of RNO at 440nm. Despite $^1\text{O}_2$ does not react chemically with RNO, the RNO bleaching is a consequence of $^1\text{O}_2$ capture by the imidazole ring, resulting in the formation of a trans-annular peroxide intermediate responsible for the bleaching of RNO as represented in **Equation 4** (52).

Equation 4: Chemical reaction leading to the bleaching of RNO.



The $\text{O}_2^{\bullet-}$ generation could be determined by the reduction of nitro blue tetrazolium (NBT) as represented in **Equation 5**; NBT can be reduced by $\text{O}_2^{\bullet-}$ via a one-electron transfer reaction, yielding partially reduced (2e^-) monoformazan (NBT^+) as a stable intermediate. Thus, $\text{O}_2^{\bullet-}$ can reduce NBT to NBT^+ , whose formation can be monitored spectrophotometrically at 560 nm.

Equation 5: Reduction of NBT to NBT^+

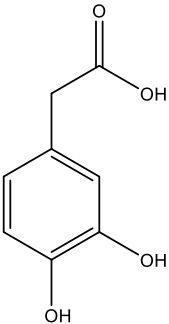
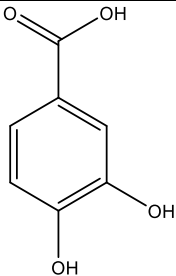
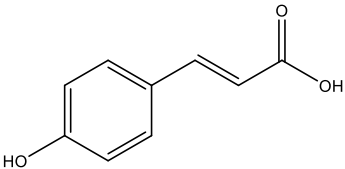


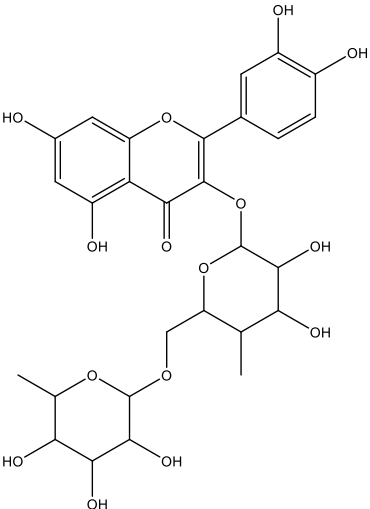
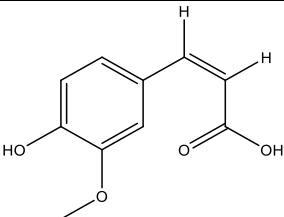
The generation of ROS may not always be involved in a phototoxic reaction since some chemicals can photobind with endogenous molecules (DNA and proteins), and photodegradants might induce toxicity directly which may lead to false negatives. With this in mind, a ROS generation assay can be used to identify the phototoxic risk of a compound but cannot prove its safety (41).

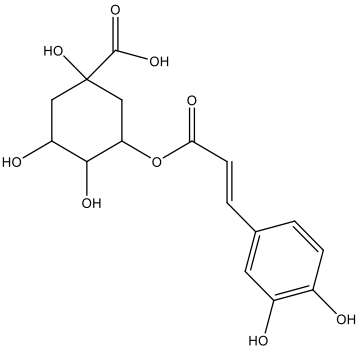
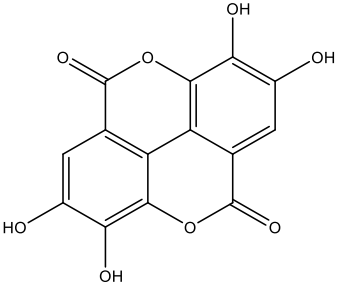
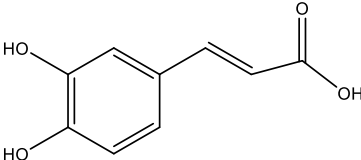
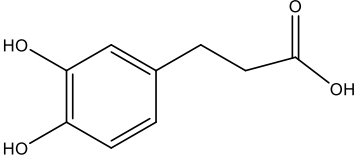
1.6 Phenolic antioxidants analyzed

Cosmetic products using natural compounds such as polyphenols are used worldwide due to their beneficial properties such as antioxidant and anti-inflammatory activities and their ability to prevent UV- induced oxidative stress and skin damage (53). In this study, compounds represented in **Table 6** that belong to the polyphenol family have been chosen. The beneficial properties of these compounds make them interesting ingredients in cosmetic formulations. Since they are present in cosmetic products and used directly on the skin, and present chromophores (that give them the ability to absorb UV radiation) they are putative phototoxic compounds.

Table 6: Information of the phenolic antioxidants analyzed.

Name	Structure	Sources	Biological Activity	Cosmetic Applications	References
3,4-dihydroxyphenylacetic acid (DOPAC)		. Predominant biologically-active catabolite of quercetin glycosides.	. Antioxidant . Anti-inflammatory	. Potential antioxidant	(54)
3,4-dihydroxybenzoic acid (Protocatechuic Acid)		. Plants such as <i>Olea europaea</i> extract and a variety of fruits and nuts.	. Antioxidant . Antimicrobial . Anti-inflammatory . Analgesic	. Anti-ageing . Anti-inflammatory . Moisturizing	(55-57)
p-Coumaric acid		. Various plants such as <i>Sasa quepaertensis nakai</i>	. Antioxidant . UV absorber . Anti-inflammatory	. Anti-ageing . Moisturizing . Anti-inflammatory	(57-60)

Rutin		. Fruits and vegetables	. Antioxidant	. Anti-ageing . Moisturizing	(57, 61, 62)
Ferulic acid		. Plants (rice, wheat, oats and pineapple), grasses, grains, vegetables, flowers, fruits, leaves, beans and more.	. Antioxidant . Antiallergic . Hepatoprotective . Anticarcinogenic . Anti-inflammatory . Antimicrobial . Antiviral . Vasodilatory . Antithrombotic	. Deodorant . Sunscreen . Anti-inflammatory	(57, 63)

<p>Chlorogenic acid</p> 	<p>. Fruits and vegetables</p>	<p>. Antioxidant . UV filter . Antimicrobial . Antimutagenic . Anti-inflammatory</p>	<p>. Anti-ageing (57, 64, 65) . Anti-inflammatory . Antibacterial</p>
<p>Ellagic acid</p> 	<p>. Numerous vegetables and fruits such as strawberries, blackberries, nuts grapes, green tea and others.</p>	<p>. Antioxidant . Antiviral . Antibacterial . Anti-inflammatory . Anticarcinogenic . Antifibrotic . Chemo protective</p>	<p>(57, 66, 67) . Anti-ageing . Whitening agent . Antibacterial . Moisturizing</p>
<p>Caffeic acid</p> 	<p>. Plants, coffee drinks, blueberries, apples and cider.</p>	<p>. Antioxidant . Antibacterial . Anticarcinogenic</p>	<p>(57, 68, 69) . Anti-ageing . Anti-inflammatory . Moisturizer</p>
<p>3,4-dihydroxyhydrocinnamic acid (Hydrocaffeic acid)</p> 		<p>. Antioxidant</p>	<p>(70) . Potential application in skin depigmentation</p>

2. AIM

The aim of this master's dissertation was to evaluate the phototoxic potential of the *Castanea Sativa* leaf extract and some of its constituents alongside with a series of raw materials for use in cosmetic products. For this purpose, a previously implemented phototoxicity assay, in a human keratinocyte cell line (HaCaT) based on the 3T3 Neutral Red Uptake Phototoxicity assay (3T3 NRU-PT) reported in OCDE₄₃₂ guideline, using a UVA/UVB Osram lamp was used. Additionally, a preliminary ROS assay was conducted to determine the photoreactivity of each compound.

3. MATERIALS AND METHODS

3.1 Materials

3.1.1 Raw materials

Ellagic acid, p-coumaric, caffeic acid, chlorpromazine hydrochloride, rutin hydrate, trans-ferulic acid, 3,4-dihydroxybenzoic acid, quercetin dihydrate, 3,4-dihydroxyhydrocinnamic acid, 3,4-dihydroxyphenylacetic acid, di-sodium hydrogen phosphate dodecahydrate, sodium phosphate monobasic monohydrate, Neutral Red (NR), chlorogenic acid and dimethyl sulfoxide (DMSO) were purchased from Sigma Aldrich. Quinine chloride, benzocaine, diclofenac and erythromycin were purchased from Acofarma. *Castanea sativa* leaf extract (*C. sativa*) was extracted by Beatriz Santos in the Laboratory of Organic and Pharmaceutical Chemistry (LQOF) of the Faculty of Pharmacy, University of Porto. The immortalized human keratinocyte (HaCaT) cell line was obtained from Cell Lines Service. DMEM with 4,5 g/L D-glucose, L-glutamine, 25mM HEPES and no phenol red, Dulbecco's Phosphate Buffered Saline (DPBS) and trypsin EDTA were purchased from Gibco. Fetal Bovine Serum was purchased from Biowest. Ethanol was supplied by Aga. N,N-dimethyl-4-nitrosoaniline (RNO), imidazole and Nitro Blue Tetrazolium (NBT) were purchased from Alfa Aesar.

3.1.2 Laboratory materials

The UVA/UVB lamp was an ultra vitalux 240V E27 from OSRAM. The laminar flow chamber (HeraSafe, class II, model HS 12), the CO₂ incubator (HERAcell 150 Air-Jacketed) Centrifuge Series (Multifuge™ X1) were from Heraeus. The Microplate Reader (Synergy HT) used to read the microplates and transform the data in images were purchased from BioTek. The inverted microscope used was a Nikon Eclipse T5100. The heating ultrasonic baths used was a Bandelin Sonorex Digetec and the Spectrophotometer Jasco UG50. The radiometer was a UVM-7 purchased from Bramédica and the freeze drier was a Crydos-80 from Telstar. The lamp used for the irradiation in the ROS assay was from Fitoclima S600PL thermostatic chamber equipped with four Repti Glo (20 W).

3.2 Methods

3.2.1 Cell culture

The *in vitro* experiments were conducted with the HaCaT cell line. These cells were originally obtained from Caucasian male aged 62 skin and are an immortal non-cancerous human keratinocyte cell line of adherent cells that form in monolayers.

The cells (passage 45 to 49) were maintained during all the assays at 37°C in a humidified atmosphere of 95% air and 5% CO₂ in the incubator in DMEM with 10% FBS and 1% antibiotics. Using an inverted microscope, cell confluence was observed and if the cells reached 70-80% confluence, subculture was done to prevent cell death. For this purpose, the culture medium was aspirated, and the cells were washed with DPBS, 2 mL of trypsin 0,25% were added and incubated for 7 to 8 min at 37°C in a 5% CO₂ atmosphere. After cell detaching, fresh medium was added to block the trypsin action. For cell counting, 10 µL of cell suspension were placed in a Neubauer chamber where the cells were counted. The obtained cell suspension was then subdivided into new flasks with fresh cell culture medium.

3.2.1.1 HaCaT cell line

In order to determinate the time necessary for the cells to duplicate, 1×10⁶ cells were seeded in five 75 cm² flasks and incubated for 24 h at 37°C in a 5% CO₂ atmosphere to reach complete adherence. Then, the cells of each flask were counted at different times. The results were plotted in a graphic representing cell number versus time, from which the doubling time was calculated using linear regression analysis.

3.2.1.2 Phototoxicity Study

The cytotoxicity of several compounds under irradiation and without irradiation in order to determine the phototoxicity was analyzed, including compounds obtained by chemical synthesis with potential interest for topical application: ellagic acid, p-coumaric acid, caffeic acid, chlorpromazine hydrochloride, rutin hydrate, trans-ferulic acid, 3,4-dihydroxyphenylacetic acid, chlorogenic acid, quinine chloride and *C. sativa* leaf extract. The tested concentrations and solvents used can be depicted in **Table 7**.

Table 7: Summary of tested compounds, solvents used, and concentrations tested.

Compounds	Solvents	Tested Concentrations
3,4-dihydroxyphenylacetic acid	DMSO	31.25; 62.5; 125; 250; 500; 1000 μ M
Caffeic acid	DMSO	12.5; 62.5; 125; 250; 500; 1000 μ M
<i>C. sativa</i> leaf extract	DMSO	5; 15.62; 25; 31.25; 62.5; 125; 250; 500 μ g/mL
Chlorogenic acid	DMSO	31.25; 62.5; 125; 250; 500 μ M
Chlorpromazine hydrochloride	DPBS	2.8; 28.2; 70.4; 140.9; 211.3; 250 μ M (Irr-) 2; 3.5; 5; 7.5; 10; 12.5 μ M (Irr+)
Ellagic acid	DMSO	12.5; 25; 50; 100; 150; 165 μ M
p-Coumaric acid	DMSO	12.5; 62.5; 125; 250; 500; 1000 μ M
Quinine chloride	ETOH 96%	300; 500; 800; 900; 950; 1000 μ M
Rutin	DMSO	31.25; 62.5; 125; 250; 500; 1000 μ M
Trans-ferulic acid	DMSO	12.5; 62.5; 125; 250; 500; 1000 μ M

With regard to cell density, 2×10^4 cells/well were seeded on 96-well tissue culture plates (150 μ L/per well) and incubated at 37°C in a 5% CO₂ atmosphere for 24 h. The medium was removed, and the different test compounds solutions prepared in DMEM without phenol red and without FBS were tested and incubated under the same conditions for 1h.

Using a radiometer, the height of the UVA/UVB Osram lamp was adjusted in order to irradiate the cells with an irradiation dose of 1.7mW/cm², which corresponds to the lamp being positioned at 35.5 cm from the plates. After this, the plate was irradiated for 10 min inside a styrofoam recipient containing a water-cooling system maintaining the temperature between 28 and 32 °C, using an equivalent plate kept in the dark. The cells were then washed once with DPBS and the medium was replaced with fresh DMEM without phenol red and incubated for 18-22h. Since the NR could precipitate, the NR

solutions were prepared every second day and incubated overnight at 37 °C in a 5% CO₂ atmosphere protected from light. At the third day, DMEM containing 50 µg/mL NR previously incubated overnight, centrifuged at 1500 g for 10 minutes and filtered (5 µm) was added to each well and incubated for 3 h under light protection. Finally, the NR solution was removed, cells were washed twice with DPBS and a desorb solution of 50% ethanol:1% acetic acid: 49% distilled water was added to extract the NR dye from the cells. The plates were then placed in a microplate shaker for 10 min, at room temperature and protected from light, to measure the absorbance at 540 nm.

The results were expressed as the absorbance ratio of treated to control cells, using **Equation 6**:

Equation 6. Cell viability (%).

$$\text{Cell viability (\%)} = \frac{\text{Treated cells absorbance}}{\text{Untreated cells absorbance}} \times 100$$

Then, the IC₅₀ was determined using a linear regression, and the PIF was calculated using the **Equation 7** (50).

Equation 7: Photo Irritation Factor (PIF).

$$PIF = \frac{IC_{50} (Irr-)}{IC_{50} (Irr+)}$$

3.2.2 *Castanea Sativa* leaf extract preparation

To obtain the *Castanea sativa* leaf extract, a hydroalcoholic solution ETOH/H₂O (7:3) was used. After extraction of the leaves and filtration, the ethanol was evaporated at 40 °C under reduced pressure. Aqueous mixtures were then frozen at -20 °C. The final step for the preparation of *C. sativa* leaf extract was freeze-drying to obtain a dry extract.

3.2.3 Spectral Absorption

As mentioned previously, the first step before conducting a phototoxicity assay is to determine if the compound absorbs UV/VIS light in the range of 290 -700 nm. Thus, the absorption spectrum of all compounds was obtained. For this purpose, the tested substances were dissolved in the appropriate solvent at a concentration of 10 µg/mL. Blanks with each solvent were performed to eliminate interferences. The solvents used for each compound were the same used at the *in vitro* cytotoxicity assays (**Table 7**).

3.2.4 ROS generation Assay

3.2.4.1 Optimization of the ROS assay

In order to optimize the ROS assay, 200 μ M quinine was tested as positive control, at different times of exposure to radiation- 1 h and 1h30min- in a controlled temperature refrigerator (25 °C).

3.2.4.2 ROS Assay

All test chemicals were prepared at a concentration of 10 mM using DMSO as solvent and protected from light.

For the $^1\text{O}_2$ determination, a reaction mixture was prepared using 9.6 mL of 20 mM sodium phosphate buffer pH 7.4 (NaPB) (5.8 g of di-sodium hydrogen phosphate dodecahydrate and 0.593 g of sodium phosphate monobasic monohydrate diluted in 1 L of purified water), 5 mL of 20 mM imidazole, 5 mL of 0.2 mM of RNO and 400 μ L of the test chemical (10 mM), and 400 μ L of DMSO for the blank determinations.

This mixture was sonicated for 5 minutes in the dark and then absorbance was read at 440 nm. After that, the mixture was transferred into a high precision cell made of Quartz to avoid absorption of UV light and was then irradiated for 1h30min. After irradiation, the absorbance was read again at 440 nm.

For the $\text{O}_2^{\bullet-}$ determination, a reaction mixture was prepared using 17.1 mL of 20 mM NaPB, 2.5 mL of 0.4 mM of NBT and 400 μ L of test chemical (10 mM), and 400 μ L of DMSO in the case of the blank.

This mixture was sonicated for 5 minutes in the dark and then absorbance was read at 560 nm. After that, the mixture was transferred into a high precision cell made of Quartz and was then irradiated for 1h30 min. After irradiation, the absorbance was read again at 560 nm.

4. RESULTS AND DISCUSSION

4.1 Spectral Absorption

All the compounds exhibited absorption in the 290-700 nm range, which according to the S10 photosafety evaluation of pharmaceuticals is a primary condition to consider a chemical for a phototoxic evaluation (47). The spectra are depicted in **figures (10-16)**.

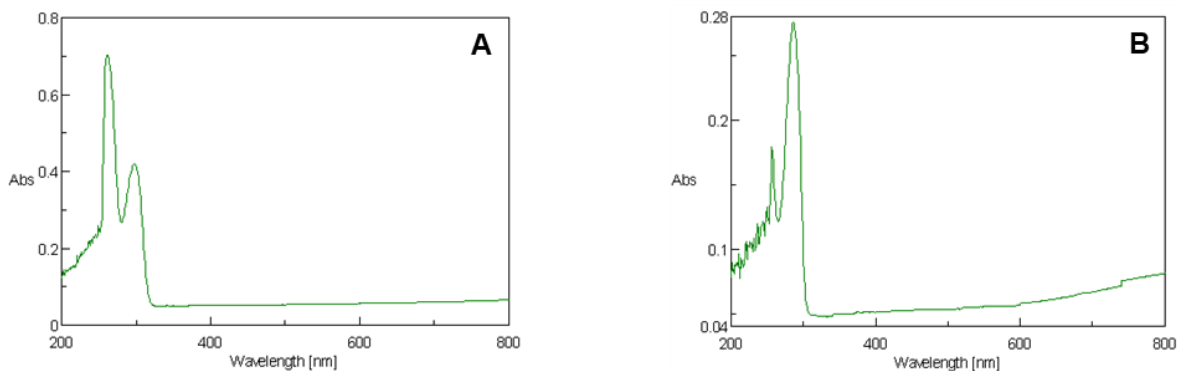


Figure 10. A) 3,4-dihydroxybenzoic acid spectral absorption and B) 3,4-dihydroxyhydrocinnamic acid spectral absorption.

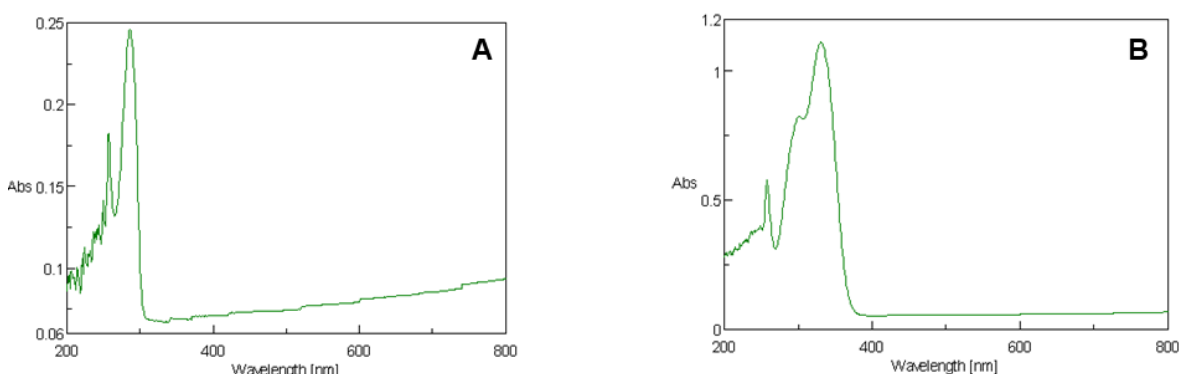


Figure 11. A) 3,4-dihydroxyphenylacetic acid spectral absorption and B) Caffeic acid spectral absorption.

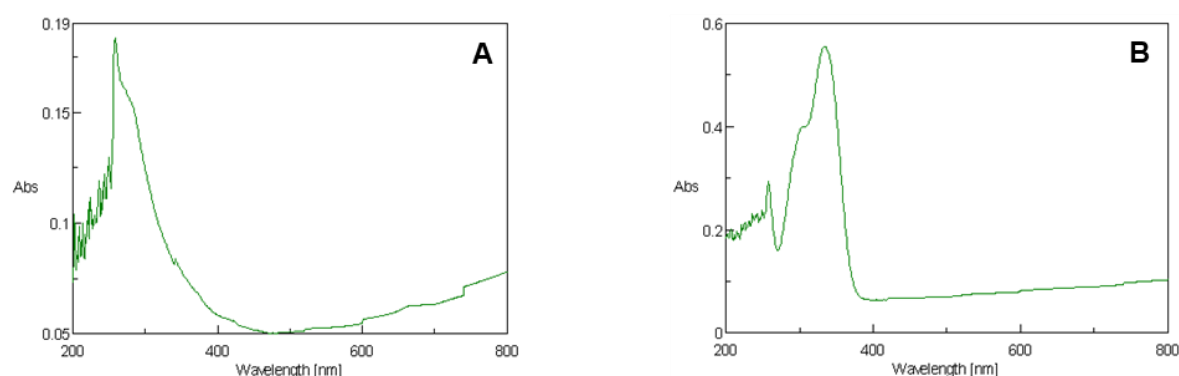


Figure 12. A) C. sativa extract spectral absorption and B) Chlorogenic acid spectral absorption.

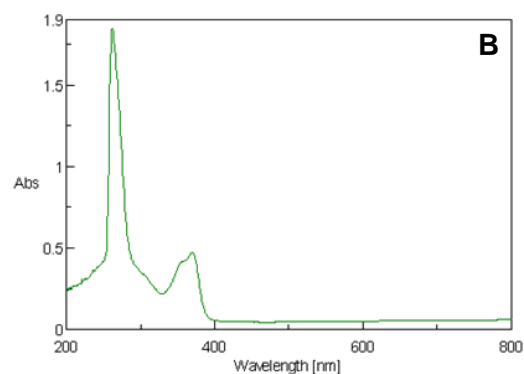
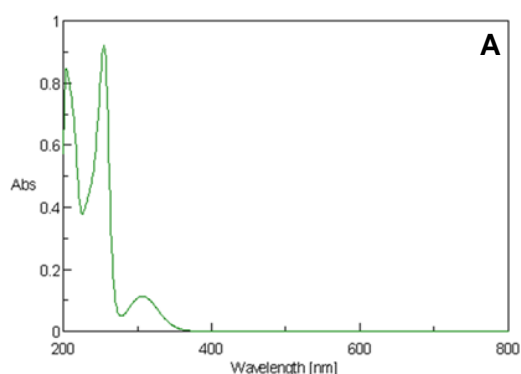


Figure 13: A) CPZ spectral absorption and B) Ellagic acid spectral absorption.

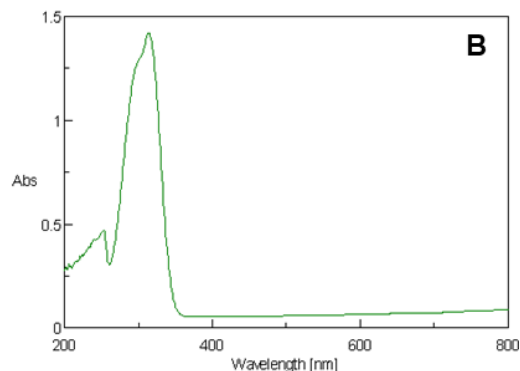
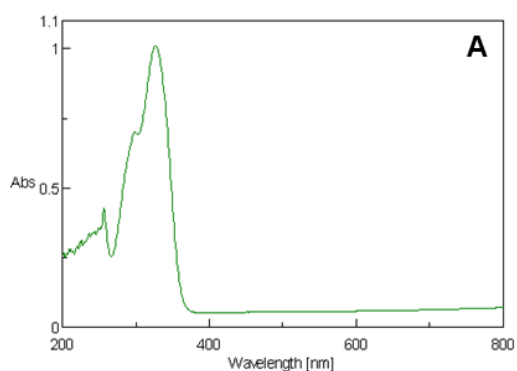


Figure 14: A) Ferulic acid spectral absorption and B) p-Coumaric acid spectral absorption.

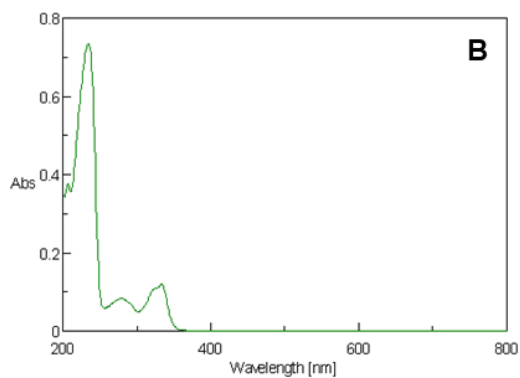
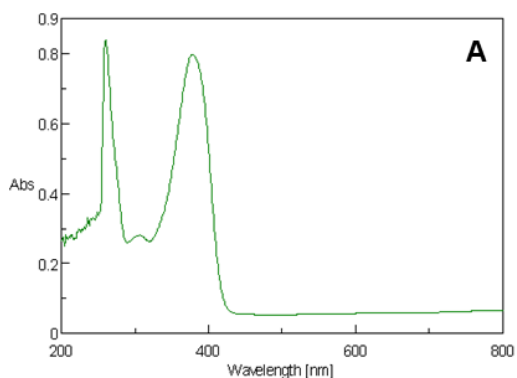


Figure 15: A) Quercetin spectral absorption and B) Quinine spectral absorption.

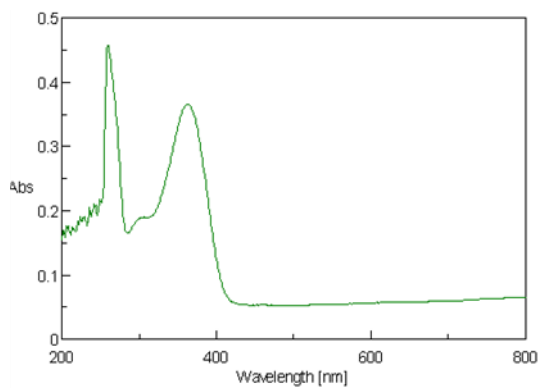


Figure 16. Rutin spectral absorption.

Since the absorbance varies with the concentration and the size of the container, for each spectrum the absorbance at the maximum wavelength was measured to determine the molar extinction coefficient (ϵ) which will compensate for this effect, by dividing the absorbance by both the concentration and the length of the solution that the light passes through. The Beer-Lambert law in **Equation 8** was used to calculate the value of ϵ allowing us to measure the probability of an electronic transition to occur.

Equation 8. Beer-lambert equation where A = Absorbance, ϵ = Molar extinction coefficient ($L\ mol^{-1}cm^{-1}$); c = concentration ($L\ mol^{-1}$); l =Length (cm)

$$A = \epsilon \times c \times l$$

In **Table 8** the value of ϵ , the λ_{max} and the absorbance obtained using the absorption spectrum of each compound are represented. Some compounds have λ_{max} inferior to 290 nm, which belong to the UVC range that does not reach the earth, and at these wavelengths, it is likely that there will be interferences due to the absorbance of the solvents.

Table 8: Molar absorptivity and maximum wavelength of the tested compounds at 10 µg/mL.

Test Compounds	$\lambda_{\max}(\text{nm})$	Absorbance	$\epsilon (\text{L mol}^{-1}\text{cm}^{-1})$
3,4-dihydroxybenzoic acid	261 and 297	$A_{261}=0.703$ $A_{297}=0.420$	$\epsilon_{261}=10835$ $\epsilon_{297}=6468$
3,4-dihydroxyhydrocinnamic acid	286	$A_{286}=0.276$	$\epsilon_{286}=5023$
3,4-dihydroxyphenylacetic acid	286	$A_{286}=0.246$	$\epsilon_{286}=4129$
Caffeic acid	331	$A_{331}=1.112$	$\epsilon_{331}=20036$
<i>C. sativa</i> leaf extract	259	$A_{259}=0.183$ $A_{290}=0.141$	NA
Chlorogenic acid	335	$A_{335}=0.556$	$\epsilon_{335}=19692$
CPZ	255 and 306	$A_{255}=0.920$ $A_{306}=0.114$	$\epsilon_{255}=32690$ $\epsilon_{306}=4047$
Ellagic acid	262 and 370	$A_{262}=1.848$ $A_{370}=0.473$	$\epsilon_{262}=55843$ $\epsilon_{370}=14287$
Ferulic acid	327	$A_{327}=1.011$	$\epsilon_{327}=19635$
p-Coumaric acid	314	$A_{314}=1.421$	$\epsilon_{314}=23335$
Quercetin	260 and 370	$A_{260}=0.840$ $A_{370}=0.798$	$\epsilon_{260}=28416$ $\epsilon_{370}=26951$
Quinine	235 and 334	$A_{235}=0.734$ $A_{334}=0.120$	$\epsilon_{235}=29138$ $\epsilon_{334}=4782$
Rutin	259 and 363	$A_{259}=0.458$ $A_{363}=0.366$	$\epsilon_{259}=27947$ $\epsilon_{363}=22354$

NA: Not applicable

The higher the value of ϵ , the more probable the electronic transition is to occur. According to the S10 photosafety evaluation of pharmaceuticals, if a compound does not have a ϵ superior to $1000 \text{ L mol}^{-1} \text{ cm}^{-1}$ it is not considered to have enough capability to absorb radiation to induce phototoxicity (47). All the compounds tested had ϵ superior to $1000 \text{ L mol}^{-1} \text{ cm}^{-1}$, which means that all are possible phototoxic compounds worth of studying. For the *C. sativa* extract it was not possible to obtain the value of ϵ since this extract contains several compounds.

4.2 ROS generation assay

To perform a ROS assay, it is first necessary to ensure irradiation conditions that satisfy the recommended criteria using a positive control, after which reference chemicals are to be tested in a feasibility study.

To ensure the selection of the appropriate condition of UV/VIS light exposure, an optimization of the ROS generation assay was performed using a positive control (quinine) and the feasibility study was conducted using some of the reference chemicals (benzocaine and erythromycin as negative reference chemicals and diclofenac and chlorpromazine hydrochloride as positive reference chemicals).

In this assay, the $^1\text{O}_2$ generation was determined by calculating the decreased absorbance of RNO at 440 nm using the **Equation 9**:

Equation 9. Equation of the decreased absorbance of RNO by singlet oxygen. Reproduced from (52).

$$\text{Decrease of A440} = [\text{A440} (-) - \text{A440} (+) - (a - b)] \times 1000$$

The $\text{O}_2^{\bullet-}$ generation was determined by calculating the increase in absorbance at 560 nm due to the formation of NBT^+ using the **Equation 10**.

Equation 10. Equation of the increased absorbance of NBT due to the formation of NBT^+ . Reproduced from (52).

$$\text{Increase of A560} = [\text{A560} (+) - \text{A560} (-) - (b - a)] \times 1000$$

For the positive control quinine, the expected values for this assay range between 319 to 583 for the $^1\text{O}_2$ and from 193 to 385 for the $\text{O}_2^{\bullet-}$. When exposed to only 1 h of irradiation, the values obtained for $^1\text{O}_2$ and $\text{O}_2^{\bullet-}$ were 191 and 102 respectively, which were below the acceptable range following this protocol. Taking into account these results, the irradiation exposure time was increased to 1h30 min in order to achieve the optimal conditions. Under these conditions, the results obtained were 354 and 234 for the $^1\text{O}_2$ and $\text{O}_2^{\bullet-}$ respectively, as represented in **Table 9**, which are within the acceptable range, thus confirming that these corresponded to the ideal test conditions. The results of all the reference chemicals were also within the acceptable range, thus proving the feasibility of this study.

All the results obtained with the ROS generation assay are represented in **Table 9**.

Using this assay, for a chemical to be considered photoreactive, the value of $^1\text{O}_2$ must be ≥ 25 and/or the value of $\text{O}_2^{\bullet-}$ must be ≥ 70 , as represented in **Figure 17**. If a chemical,

after irradiation, has the ability to generate one of these reactive oxygen species, it is considered photoreactive.

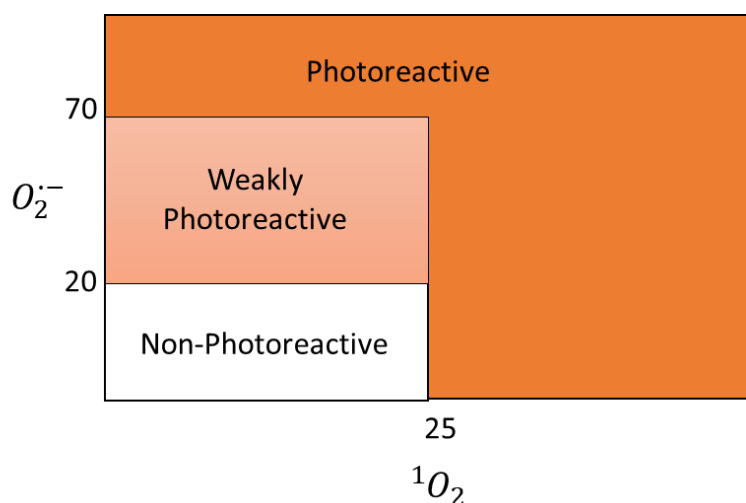


Figure 17: Photoreactivity criteria for the ROS assay. Adapted from (52).

Table 9: Summary of the results obtained for each compound using the ROS generation assay.

Compounds	1O_2	$O_2^{\bullet -}$	Photoreactivity
Quinine	354	234	Photoreactive
Diclofenac	443	510	Photoreactive
Erythromycin	1	6	Non-photoreactive
Benzocaine	3	-2	Non-photoreactive
Chlorpromazine Hydrochloride	-212	120	Photoreactive
Caffeic Acid	-2	4	Non-photoreactive
Ferulic Acid	-9	-1	Non-photoreactive
Rutin	15	12	Non-photoreactive
p-Coumaric Acid	-3	2	Non-photoreactive
Quercetin	Precipitation	Precipitation	Inconclusive
3,4-dihydroxybenzoic Acid	-5	6	Non-photoreactive
3,4-dihydroxyhydrocinnamic Acid	3	1	Non-photoreactive
Ellagic Acid	Precipitation	Precipitation	Inconclusive
3,4-dihydroxyphenylacetic Acid	38	4	Photoreactive
C. Sativa leaf extract	100	Precipitation	Photoreactive

With this assay, it was possible to conclude that quinine and diclofenac are photoreactive generating both $^1\text{O}_2$ and $\text{O}_2^{\bullet-}$. Chlorpromazine hydrochloride was considered photoreactive, based on the generation of only $\text{O}_2^{\bullet-}$. For the *C. sativa* leaf extract, $^1\text{O}_2$ was generated, and precipitation was detected in the $\text{O}_2^{\bullet-}$ generation. Since $^1\text{O}_2$ was generated, even though the $\text{O}_2^{\bullet-}$ generation test could not be concluded for the *C. sativa* leaf extract, it is still considered photoreactive because it does generate $^1\text{O}_2$. All other compounds, erythromycin, benzocaine, caffeic acid, ferulic acid, rutin, p-coumaric acid, 3,4-dihydroxybenzoic acid and 3,4-dihydroxyhydrocinnamic acid tested negative in this assay, which means they don't generate reactive oxygen species when irradiated under these test conditions. Since the mechanisms of phototoxicity are not only based on the generation of ROS, the results from this assay can lead to false negatives because, if a compound is photoactivated and reacts directly with DNA or proteins it will lead to phototoxicity, without generating ROS. Further *in vitro* studies should be performed to confirm these results. Both ellagic acid and quercetin precipitated in both tests making them incompatible with the ROS assay so no conclusions referring to their photoreactivity can be taken.

In the case of 3,4-dihydroxyphenylacetic acid (DOPAC), surprisingly $^1\text{O}_2$ was generated leading to the conclusion that it is photoreactive. These results were unexpected since the chemical structure of DOPAC is very similar to the 3,4-dihydroxyhydrocinnamic acid and to the 3,4-dihydroxybenzoic acid which are not photoreactive. More studies are required in order to understand why DOPAC is photoreactive, but this might be a start to determine a correlation between the chemical structure and the potential of a chemical to be photoreactive.

4.3 Neutral red uptake phototoxicity assay

4.3.1 HaCaT cell line characterization

The doubling time of the HaCaT cell line reported in the literature is of 26 h (71). In order to confirm that the HaCaT cell line used for the phototoxicity assays was in normal test conditions, the doubling time of the HaCaT cell line was determined by linear regression analysis as depicted in **Figure 18**. The calculated doubling time obtained was of 20.43 h thus conforming that the cells used were in normal growth conditions.

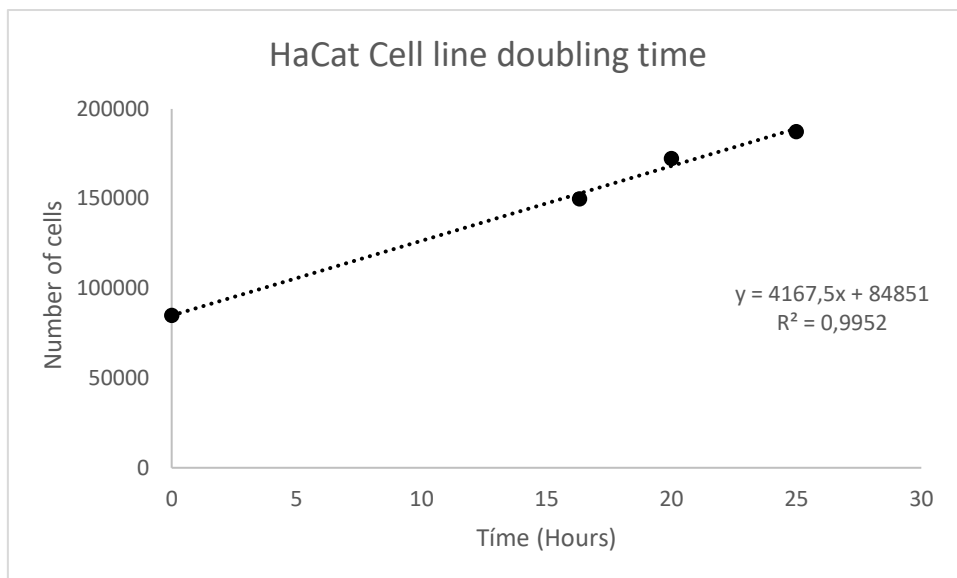


Figure 18: Determination of HaCat cell line doubling time by linear regression analysis.

4.3.2 Solvent control

The cytotoxicity of all solvents used for the evaluation of phototoxic effects, in the presence and absence of irradiation, after 1h of exposure is depicted in **Figure 19** and **Figure 20**.

For the non-irradiated plate, these solvents did not show a statistically significant difference relative to the negative controls. However, for the irradiated plate, there is a significant difference between the 1% DMSO and 2% ethanol solvent controls relative to the negative controls, which justifies the use of solvent controls on all experiments.

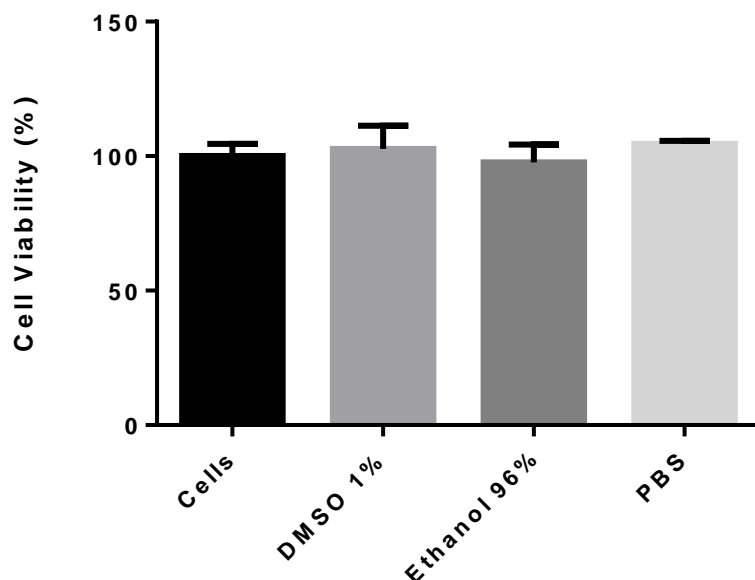


Figure 19: Cell viability of HaCaT cell line exposed to solvent by the Neutral Red assay. Data are presented as mean \pm SD (n=3). Data were analyzed using One-way ANOVA with Dunnett post hoc test.

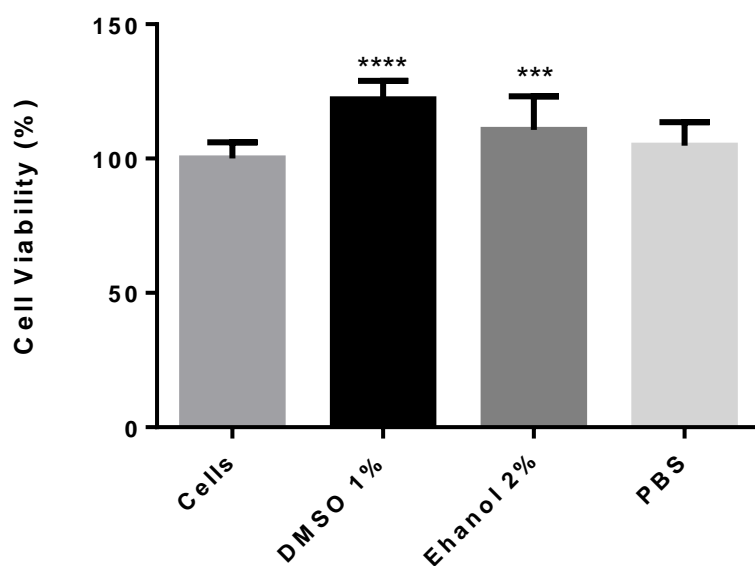


Figure 20: Cell viability of HaCaT cell line exposed to solvent control by the Neutral Red assay after irradiation. Data are presented as mean \pm SD (n=3). Data were analyzed using One-way ANOVA with Dunnett post hoc test. **** $p < 0.0001$ vs. Cells *** $p < 0.001$.

4.3.3 Positive controls

4.3.3.1 Chlorpromazine

Chlorpromazine is the most frequently used positive control for phototoxicity assays (50). Under our test conditions, the IC₅₀ (Irr+) obtained was 4.83 ± 0.77 μ M and

the IC₅₀ (Irr-) obtained was $86.19 \pm 12.01 \mu\text{M}$. The calculated PIF value corresponds to 17.89 ± 1.37 . These results show that CPZ is phototoxic to the tested keratinocyte cell line. As previously demonstrated in the ROS assay, CPZ also generates ROS when irradiated, which supports these conclusions, as was expected since reports of its *in vivo* phototoxicity are available in the literature (45).

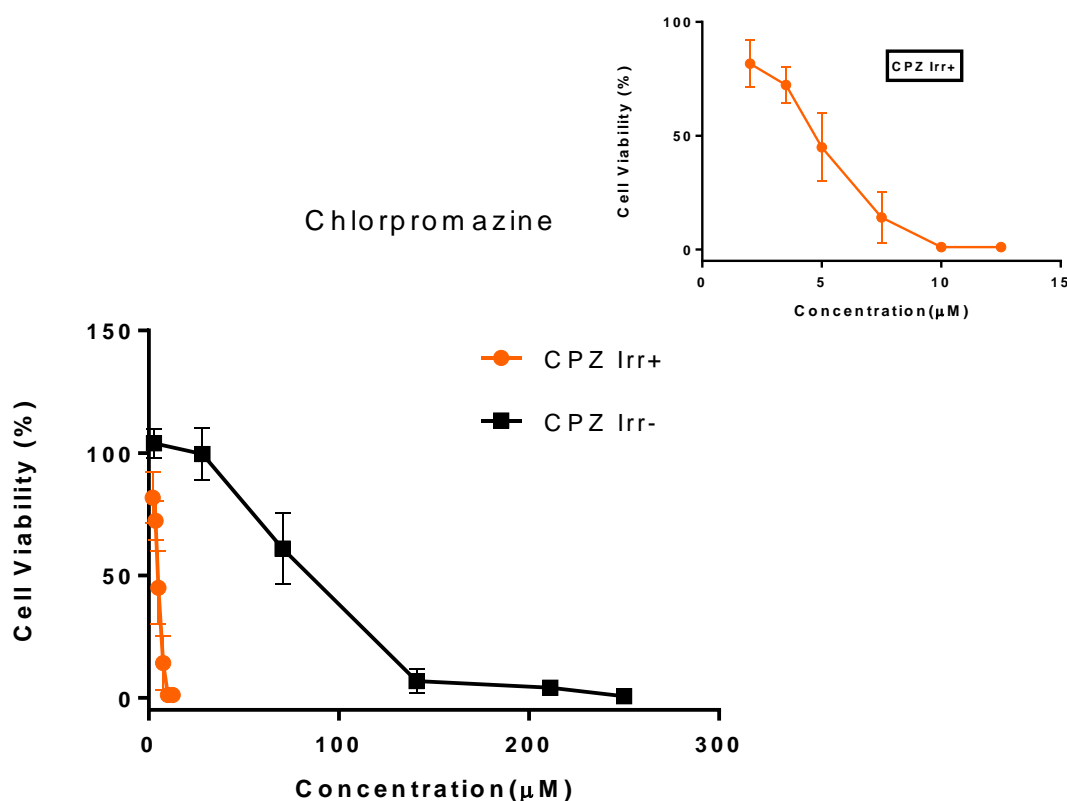


Figure 21: Cell viability of HaCaT cell line exposed to chlorpromazine, determining the phototoxicity by the Neutral Red assay. Irr-: Non-irradiated. Irr+: Irradiated plate. Data are presented as mean \pm SD ($n=3$) relative to solvent control.

4.3.3.2 Quinine

Quinine is also frequently tested as a positive control in phototoxicity assays (45). In this study, the IC₅₀ (Irr+) obtained was $599.63 \pm 38.96 \mu\text{M}$ and the IC₅₀ (Irr-) was $664.56 \pm 37.23 \mu\text{M}$, so the value of PIF calculated was $1.11 \pm 0.01 \mu\text{M}$. Even though quinine tested positive in the ROS assay, generating both $^1\text{O}_2$ and $\text{O}_2^{\cdot-}$, these results show that quinine has no phototoxic effect on the keratinocyte cell line. These results can be justified by the powerful antioxidant defense system present in the keratinocytes, when compared to the fibroblasts, leading to the conclusion that the keratinocytes

antioxidant defense system has the ability to neutralize the ROS generated by quinine when irradiated. Although quinine was considered phototoxic in the 3T3 NRU PT, quinine has not yet shown convincing evidence for an *in vivo* phototoxic effect (72) which leads to the conclusion that a keratinocyte human cell line might be a more representative of the human *in vivo* situation when compared to the Balb/c 3T3 cell line, that corresponds to mouse fibroblasts. Nevertheless, is still worth mentioning that quinine induces photoallergic responses in some individuals (72).

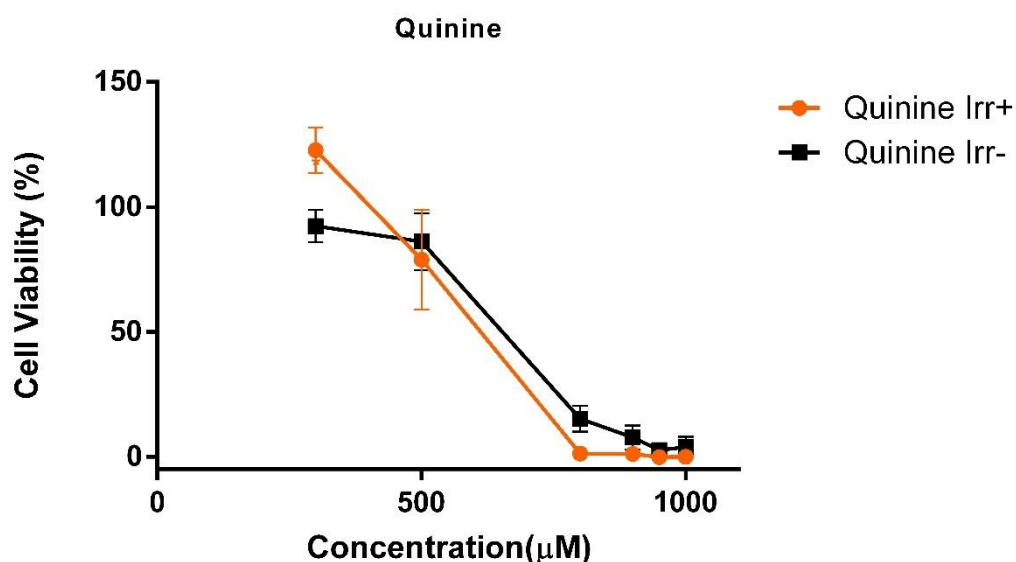


Figure 22: Cell viability of HaCaT cell line exposed to quinine, determining the phototoxicity by the Neutral Red assay. Irr-: Non-irradiated. Irr+: Irradiated plate. Data are presented as mean \pm SD ($n=3$) relative to solvent control.

4.3.4 Raw Materials

4.3.4.1 Caffeic acid

Caffeic acid did not show toxicity in this concentration range, making it impossible to determine the IC₅₀ and PIF values. However, after analyzing the results, it is possible to perceive a dose-dependent increase in cell viability until a plateau is reached at 125 μM. With these results and the fact that caffeic acid tested negative in the ROS generation assay it is possible to conclude that caffeic acid is not phototoxic. These results are not different from what was expected since caffeic acid has already shown photoprotective properties against UV-mediated oxidative damage. Since UV radiation

leads to the generation of ROS and depletion of antioxidant defenses in keratinocytes, the antioxidant properties of caffeic acid were expected to inhibit this damage (68, 73).

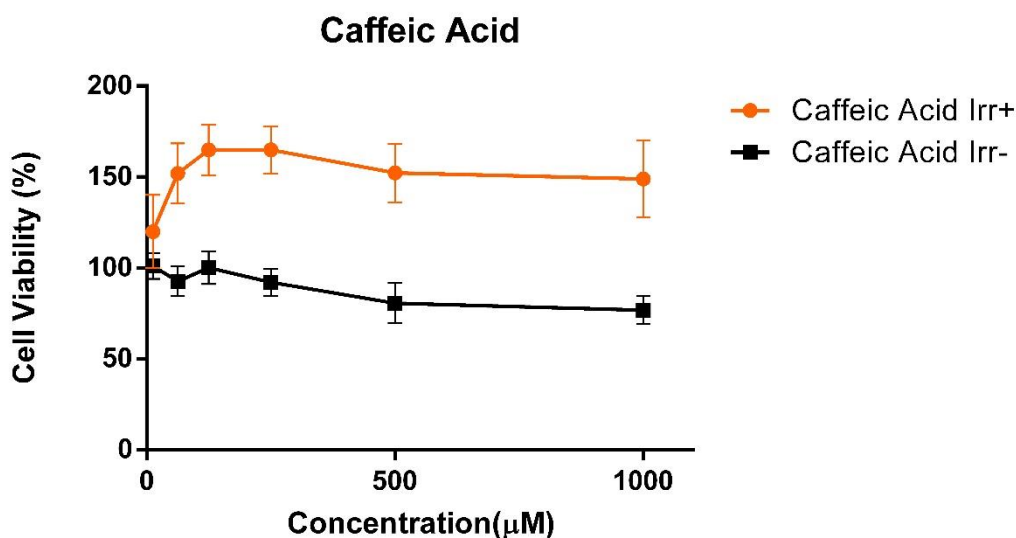


Figure 23: Cell viability of HaCaT cell line exposed to caffeic acid, determining the phototoxicity by the Neutral Red assay. Irr-: Non-irradiated. Irr+: Irradiated plate. Data are presented as mean \pm SD (n=3) relative to solvent control.

4.3.4.2 Ferulic acid

Ferulic acid results, similar to what was observed for caffeic acid, did not allow to determine the IC₅₀ and PIF values, due to the absence of a cytotoxic effect. It is still possible to observe a dose-dependent increase in viability until a plateau is reached at 125 μM, and ferulic acid also tested negative in the ROS generation assay leading to the conclusion that ferulic acid is also not phototoxic. Just like caffeic acid, these results were expected since reports had shown that ferulic acid also has photoprotective properties due to its antioxidant properties and did not show cytotoxicity in HaCaT cells (73).

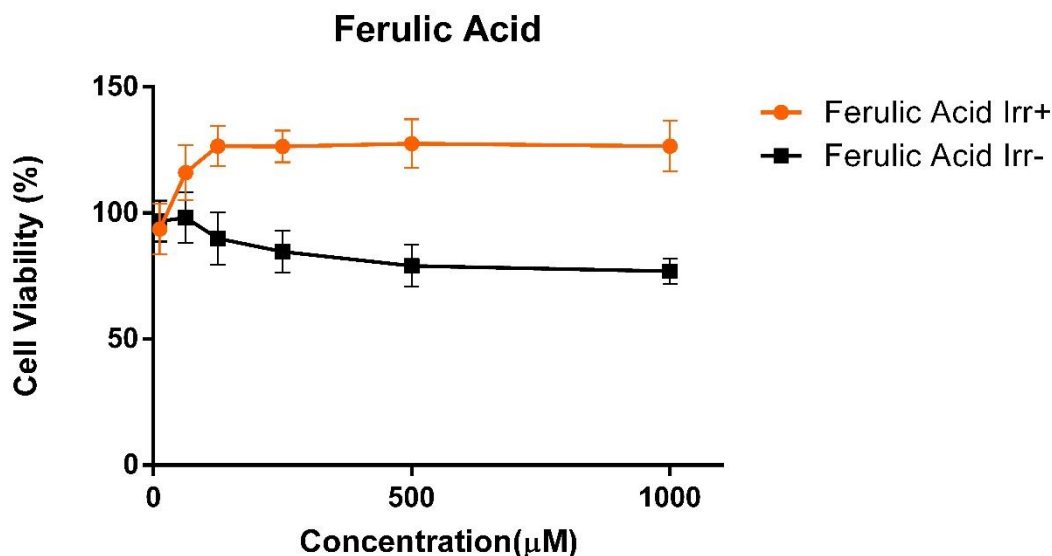


Figure 24: Cell viability of HaCaT cell line exposed to ferulic acid, determining the phototoxicity by the Neutral Red assay. Irr-: Non-irradiated. Irr+: Irradiated plate. Data are presented as mean \pm SD (n=3) relative to solvent control.

4.3.4.3 p-Coumaric acid

Similar to caffeic acid and to ferulic acid, p-coumaric acid did not show toxicity in this concentration range making it impossible to determine the IC₅₀ and PIF values. Again, a dose-dependent increase in viability was detected until a plateau is reached at 500 μ . Since p-coumaric acid also tested negative in the ROS assay it is possible to conclude that p-coumaric acid is not phototoxic. Some studies have also documented the antioxidant properties of p-coumaric acid (59) and its ability to attenuate UVB-induced cell death of HaCaT cells supporting the results obtained in this work (58).

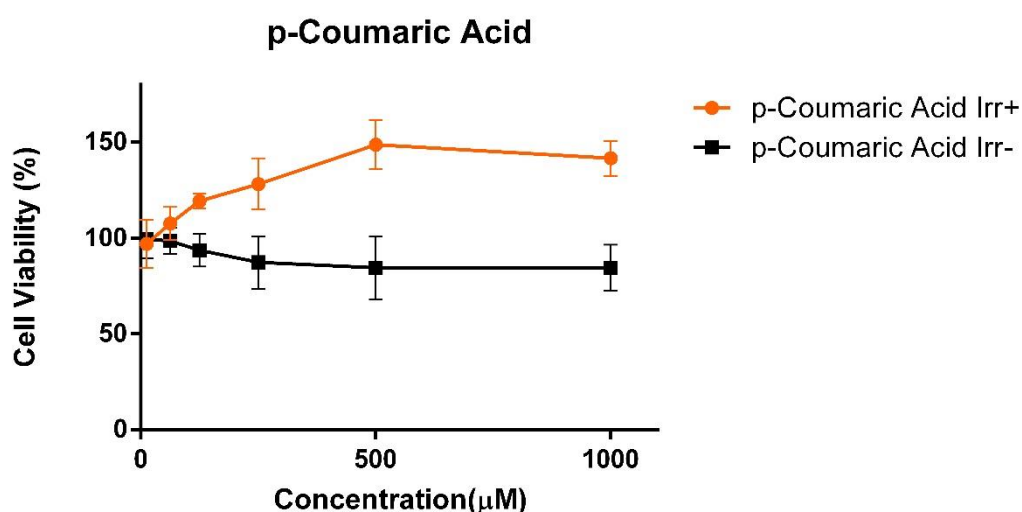


Figure 25: Cell viability of HaCaT cell line exposed to p-coumaric acid, determining the phototoxicity by the Neutral Red assay. Irr-: Non-irradiated. Irr+: Irradiated plate. Data are presented as mean \pm SD (n=3) relative to solvent control.

4.3.4.4 3,4-dihydroxyphenylacetic acid (DOPAC)

3,4-dihydroxyphenylacetic acid (DOPAC) in this concentration range did not reach 50% of cell death so it was impossible to determine the IC₅₀ and consequently the PIF value. This compound tested positive in the ROS assay, generating oxygen singlet however, it showed no phototoxic potential in HaCaT cell line. This might be again explained by the keratinocyte's antioxidant defense system which might be able to neutralize the ROS generated by the UV irradiation of this compound. Another explanation might be to the differences between the irradiation conditions in the ROS assay and the *in vitro* assay since the irradiation emitted in the ROS assay includes some wavelengths inferior to 290 nm *in vitro* assay may not. Since the spectrum of DOPAC shows a maximum absorbance peak at 286 nm this might explain why DOPAC generated ROS but did not induce phototoxicity *in vitro*. Reports have shown that DOPAC has antioxidant activity and promotes an enhancement of the total glutathione activity which might explain the results obtained in this assay (54).

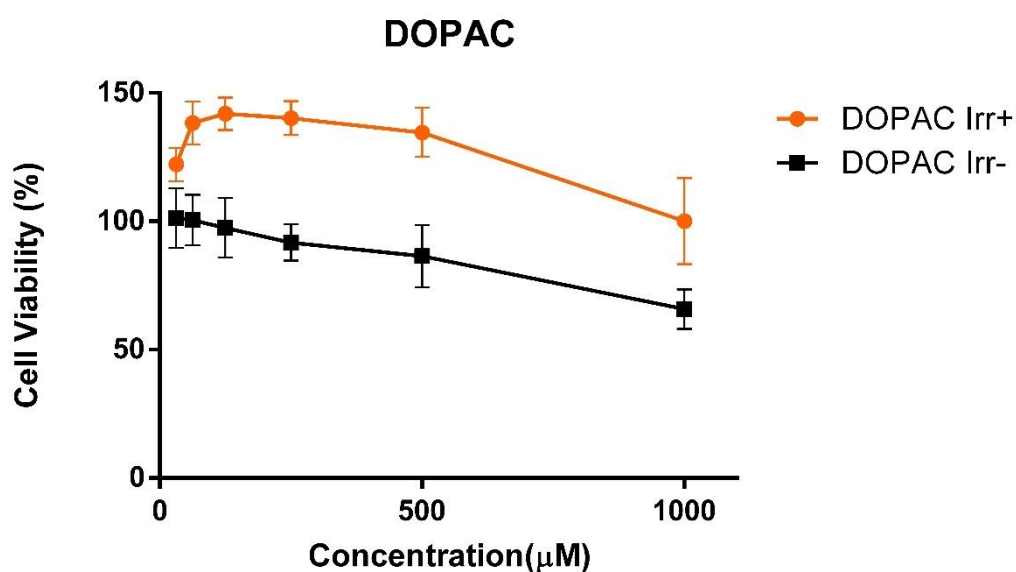


Figure 26: Cell viability of HaCaT cell line exposed to 3,4-dihydroxyphenylacetic acid, determining the phototoxicity by the Neutral Red assay. Irr-: Non-irradiated. Irr+: Irradiated plate. Data are presented as mean \pm SD ($n=3$) relative to solvent control.

4.3.4.5 *Castanea sativa* leaf extract

The results obtained for the *C. sativa* leaf extract revealed an IC₅₀ (Irr+) of 17.86 \pm 2.35 μg/mL and an IC₅₀ (Irr-) of 213.13 \pm 23.23 μg/mL. The PIF value obtained was 12.00 \pm 1.04 leading to the conclusion that the *C. sativa* leaf extract is phototoxic to the HaCaT cells. The results obtained in the ROS assay support this conclusion since it

tested positive in the generation of ROS. Additionally, our research group performed previously *in vivo* studies (unpublished data) suggesting that the *C. sativa* extract exerts phototoxicity in humans.

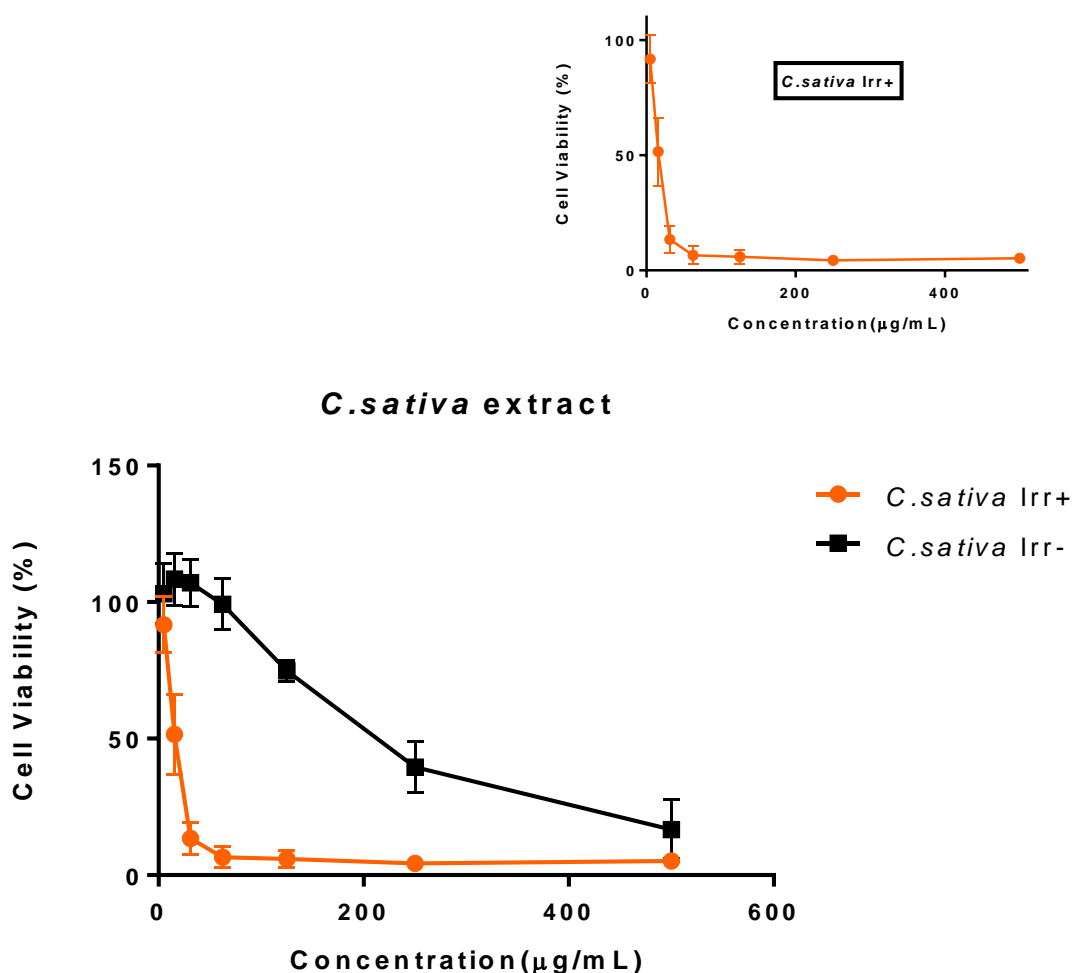


Figure 27: Cell viability of HaCaT cell line exposed to *Castanea sativa* extract, determining the phototoxicity by the Neutral Red assay. Irr-: Non-irradiated. Irr+: Irradiated plate. Data are presented as mean \pm SD ($n=3$) relative to solvent control.

4.3.4.6 Chlorogenic acid

Chlorogenic acid (CA) is a phenolic compound present in *C. sativa* leaf extract. No toxicity was shown under the test conditions, so it was impossible to determine the IC₅₀ and PIF values. Since an increase in viability was shown in this assay, it is possible to conclude that CA is not phototoxic. In *C. sativa* extract there are 2.81mg of CA/g (32) so, in a concentration of 500 µg/mL of extract a maximum 3.965 µM CA concentration is

expected. Since the range of concentrations tested was higher than the concentration of CA present in the extract, is possible to conclude that CA, by itself is not responsible for the phototoxicity observed for the extract. CA antioxidant properties have been already reported and CA also has shown to be able to reduce the amount of DNA breakage induced by UVB radiation which occurs via the generation of ROS thus confirming our results (74).

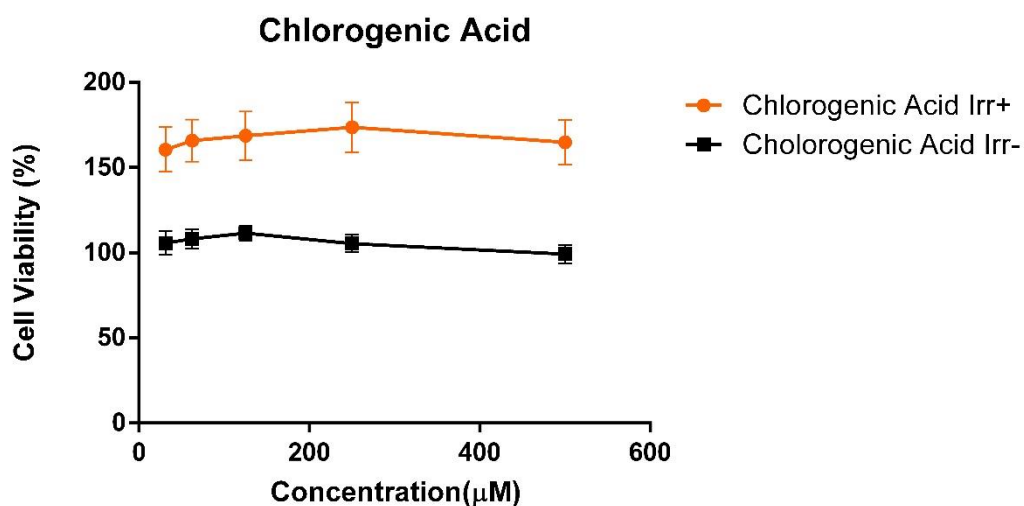


Figure 28 Cell viability of HaCaT cell line exposed to chlorogenic acid, determining the phototoxicity by the Neutral Red assay. Irr-: Non-irradiated. Irr+: Irradiated plate. Data are presented as mean \pm SD (n=3) relative to solvent control.

4.3.4.7 Ellagic acid

Ellagic acid, like CA, is present in the *C. sativa* leaf extract. As with CA, it did not show toxicity in this concentration range making it impossible to determine the IC₅₀ and PIF values. Although it was not possible to determine the photoreactivity of ellagic acid with the ROS assay, with these results it is possible to observe an increase in cell viability for the irradiated cells in the presence of ellagic acid. Due to solubility issues, it was impossible to test higher concentrations of this compound. However, taking into account that there are 4.20 mg of ellagic acid/g extract (32), in a concentration of 500 μg/mL of extract a maximum concentration of 2.1 μg/mL of ellagic acid is expected. This corresponds to 6.95 μM of ellagic acid, so it can be concluded that ellagic acid by itself is not responsible for the phototoxicity of the extract, since it is not phototoxic up to 165 μM and the extract, at 500 μg/mL presented 100% mortality for the irradiated and non-irradiated cells. Ellagic acid has shown antioxidant activity in other studies and ability to attenuate the intracellular ROS levels in fibroblasts under UVB-induced oxidative stress, thus confirming our results (66).

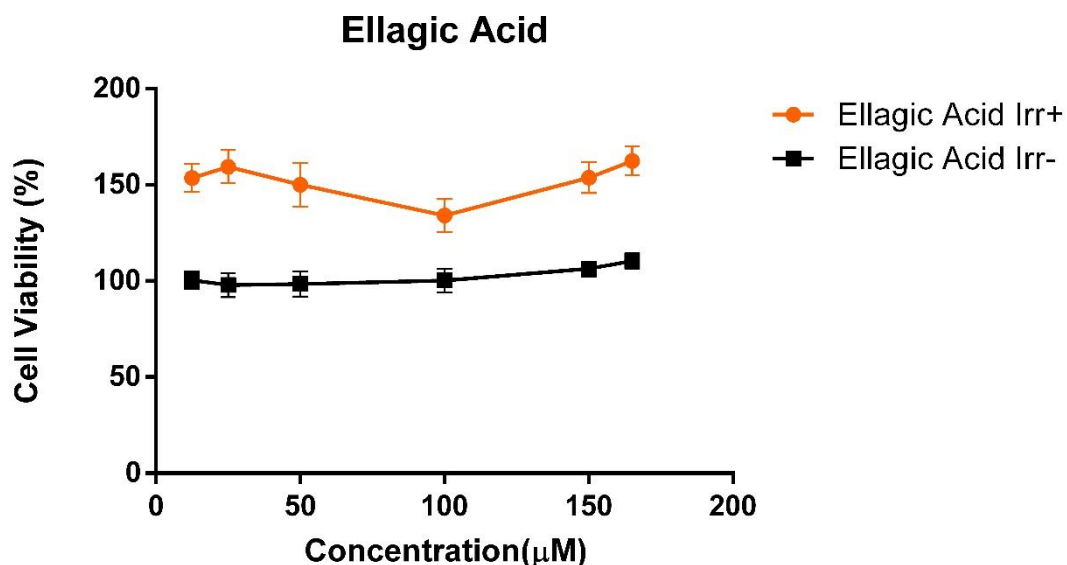


Figure 29: Cell viability of HaCaT cell line exposed to ellagic acid, determining the phototoxicity by the Neutral Red assay. Irr-: Non-irradiated. Irr+: Irradiated plate. Data are presented as mean \pm SD (n=3) relative to solvent control.

4.3.4.8 Rutin

Rutin is the most abundant phenolic compound in the *C. sativa* leaf extract. It was impossible to determine the IC₅₀ and PIF values due to the lack of cytotoxicity for the tested concentration range. The results showed an increase in viability when the cells are irradiated in the presence of rutin and taking also into account the negative results for the generation of ROS, it is possible to conclude that rutin is not phototoxic. Considering that *C. sativa* extract contains only 16 mg of rutin/g extract (32), and since the range of concentrations tested exceeds this concentration, it is safe to conclude that rutin, by itself, is not responsible for the phototoxicity of the extract. Rutin has shown high radical scavenging activity and antioxidant activity which support the results obtained in this study (61).

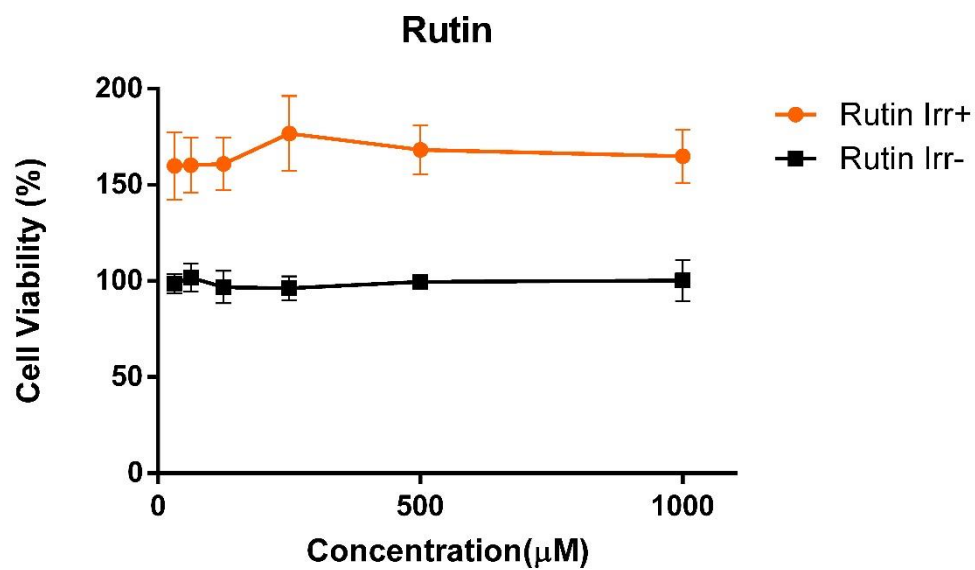


Figure 30: Cell viability of HaCaT cell line exposed to rutin, determining the phototoxicity by the Neutral Red assay. Irr-: Non-irradiated. Irr+: Irradiated plate. Data are presented as mean \pm SD (n=3) relative to solvent control.

In **Table 10** the results obtained for the neutral red uptake phototoxicity assay and ROS assay are summarized.

Table 10: Summary of data obtained with the phototoxicity and ROS generation assays.

Compound	IC50(Irr+)	IC50 (Irr-)	PIF	ROS assay	Phototoxic potential
3,4-dihydroxyphenylacetic acid	NA	NA	NA	P	Not phototoxic
Caffeic acid	NA	NA	NA	NP	Not phototoxic
<i>C. sativa</i> extract	17.86 ± 2.35 µg/mL	213.13 ± 23.23 µg/mL	12.00 ± 1.04	P	Phototoxic
Chlorogenic acid	NA	NA	NA	-	Not phototoxic
CPZ	4.83 ± 0,77 µM	86.19 ± 12.01 µM	17.89 ± 1.37	P	Phototoxic
Ellagic acid	NA	NA	NA	I	Not phototoxic
Ferulic acid	NA	NA	NA	NP	Not phototoxic
p-Coumaric acid	NA	NA	NA	NP	Not phototoxic
Quinine	599.63 ± 38.96 µM	664.56 ± 37.23 µM	1.11 ± 0.01	P	Not phototoxic
Rutin	NA	NA	NA	NP	Not phototoxic

NA: Not applicable. P: Photoreactive. NP: Not-photoreactive. I: Inconclusive

5. CONCLUSIONS

In the early stages of drug discovery, evaluating the photosafety of a chemical is of high importance since it can prevent the appearance of undesirable drug reactions and is currently a requisite for all drug products. In particular, photosafety evaluation is of special interest for cosmetic products because they are intended to be applied on the skin surface, and therefore exposed to the sunlight. Since animal testing has been banned for cosmetics products, alternative methodologies have been developed in order to evaluate the phototoxic potential of cosmetic ingredients such as the 3T3 Neutral Red Uptake Phototoxicity assay (3T3 NRU-PT) reported in OCDE₄₃₂ guideline that is currently recommended. However, this *in vitro* methodology uses a mouse cell line and various studies reported that is over-sensitive leading to a high number of false positives when compared to the results *in vivo*.

With these limitations in mind, in this work a methodology based on the 3T3 NRU-PT methodology but using a human keratinocyte cell line (HaCaT) was applied. Since this methodology used human keratinocyte cells, a more realistic model was expected, given that these are the most abundant type of cells present in the external layer of the skin, where the topical compounds would be applied and exposed to the sun radiation.

The PIF value for CPZ was 17.89 ± 1.37 , confirming its phototoxicity in the present study model. However, for quinine, the calculated PIF value was surprisingly of 1.11 ± 0.01 , leading to the conclusion that quinine is not phototoxic in the keratinocyte cell line. This may be explained due to the keratinocytes' superior antioxidant defense system being able to neutralize the ROS generated by quinine when irradiated. Since convincing *in vivo* evidence of quinine phototoxicity has not yet been reported, these results support the idea that the human keratinocyte cell line may be more realistic when compared to the Balb/c 3T3 mouse fibroblast cell line.

All compounds tested absorbed radiation in the 290-700 nm range with ϵ values higher than $1000 \text{ M}^{-1} \text{ cm}^{-1}$ thus indicating a possible phototoxic potential.

A ROS generation assay demonstrated that 3,4-dihydroxyphenylacetic acid, quinine, diclofenac, chlorpromazine hydrochloride and *C. sativa* extract were photoreactive. In contrast, erythromycin, benzocaine, caffeic acid, ferulic acid, rutin, p-coumaric acid, 3,4-dihydroxybenzoic acid and 3,4-dihydroxyhydrocinnamic acid were not photoreactive. Since the mechanisms of phototoxicity are not only based on the generation of ROS, the results from this assay can lead to false negatives because if a compound is photoactivated and reacts directly with DNA or proteins it will lead to

phototoxicity, without generating ROS. For this reason, this assay is considered insufficient to determine the phototoxic potential of a chemical.

3,4-dihydroxyphenylacetic acid (DOPAC) tested photoreactive in the ROS assay so it was interesting to test its phototoxic potential *in vitro*. The results showed no phototoxic potential in the HaCaT cell line. Like quinine, this might be explained by the keratinocytes' antioxidant defense system. These differences may also come from the different light sources that DOPAC was exposed.

Caffeic, ferulic and p-coumaric acid are frequently used ingredients in the cosmetic industry and all of them revealed to be not phototoxic and not photoreactive.

With this work it was possible to conclude that the *C. sativa* leaf extract is photoreactive in the ROS assay, and phototoxic in the HaCaT cell line with a PIF value of 12.00 ± 1.04 . We explored the possibility of some of its constituents to be phototoxic but chlorogenic acid, ellagic acid and rutin, all identified phenolic antioxidants on the extract, were not phototoxic.

Natural extracts such as *C. sativa* are very complex and thus understanding the cause of their phototoxic effect is a challenging task. For further elucidation of the phototoxicity induced by the *C. sativa* extract it would be interesting to study other compounds like hiperoside and isoquercitrin and the presence of metals such as copper and iron that are well known ROS-generators. Another approach would be the design of experiments aiming at studying interaction of the different compounds present in the extract.

6. REFERENCES

1. Martin MT, Vulin A, Hendry JH. Human epidermal stem cells: Role in adverse skin reactions and carcinogenesis from radiation. *Mutation research*. 2016;770(Pt B):349-68.
2. Trouba KJ, Hamadeh HK, Amin RP, Germolec DR. Oxidative stress and its role in skin disease. *Antioxid Redox Signal*. 2002;4(4):665-73.
3. Aburjai T, Natsheh FM. Plants used in cosmetics. *Phytother Res*. 2003;17(9):987-1000.
4. Dzialo M, Mierziak J, Korzun U, Preisner M, Szopa J, Kulma A. The Potential of Plant Phenolics in Prevention and Therapy of Skin Disorders. *International journal of molecular sciences*. 2016;17(2):160.
5. Smart Servier Medical Art. Skin [Available from: https://smart.servier.com/smart_image/skin/]. [26 September 2018].
6. Baroni A, Buommino E, De Gregorio V, Ruocco E, Ruocco V, Wolf R. Structure and function of the epidermis related to barrier properties. *Clinics in dermatology*. 2012;30(3):257-62.
7. Wickett RR, Visscher MO. Structure and function of the epidermal barrier. *American Journal of Infection Control*. 2006;34(10):S98-S110.
8. Ribeiro A, Estanqueiro M, Oliveira M, Sousa Lobo J. Main Benefits and Applicability of Plant Extracts in Skin Care Products. *Cosmetics*. 2015;2(2):48-65.
9. Anny Fournanier DMaSS. Sunscreens containing the broad-spectrum UVA absorber, Mexoryls SX, prevent the cutaneous detrimental effects of UV exposure: a review of clinical study results. 2008.
10. Mattavelli I, Patuzzo R, Torri V, Gallino G, Maurichi A, Lamera M, et al. Prognostic factors in Merkel cell carcinoma patients undergoing sentinel node biopsy. *Eur J Surg Oncol*. 2017.
11. Lopes MB, Rajasekaran R, Lopes Cancado AC, Martin AA. In vivo Confocal Raman Spectroscopic Analysis of the Effects of IR Radiation in the Human Skin Dermis. *Photochemistry and photobiology*. 2016.
12. Rinnerthaler M, Bischof J, Streubel MK, Trost A, Richter K. Oxidative stress in aging human skin. *Biomolecules*. 2015;5(2):545-89.
13. Dasuri K, Zhang L, Keller JN. Oxidative stress, neurodegeneration, and the balance of protein degradation and protein synthesis. *Free radical biology & medicine*. 2013;62:170-85.

14. Birch-Machin MA, Bowman A. Oxidative stress and ageing. *Br J Dermatol*. 2016;175 Suppl 2:26-9.
15. Dyke HKaKV. Oxidative and Nitrosative Stresses: Their Role in Health and Disease in Man and Birds. *Oxidative Stress - Molecular Mechanisms and Biological Effects*2012.
16. Birben E, Sahiner UM, Sackesen C, Erzurum S, Kalayci O. Oxidative stress and antioxidant defense. *World Allergy Organ J*. 2012;5(1):9-19.
17. Lushchak VI. Free radicals, reactive oxygen species, oxidative stress and its classification. *Chemico-biological interactions*. 2014;224:164-75.
18. Souza C, Campos P. Development and photoprotective effect of a sunscreen containing the antioxidants Spirulina and dimethylmethoxy chromanol on sun-induced skin damage. *Eur J Pharm Sci*. 2017;104:52-64.
19. Gregus Z. Casarett and doull's toxicology the basic science of poisons. In: Klaassen CD, editor.2007. p. 86.
20. Kammeyer A, Luiten RM. Oxidation events and skin aging. *Ageing Res Rev*. 2015;21:16-29.
21. Ogilvie APaBW. Casarett and doull's toxicology the basic science of poisons. In: Klaassen CD, editor.2007.
22. Stohs SJ, Bagchi D. Oxidative mechanisms in the toxicity of metal ions. *Free radical biology & medicine*. 1995;18(2):321-36.
23. Karran P, Brem R. Protein oxidation, UVA and human DNA repair. *DNA Repair (Amst)*. 2016;44:178-85.
24. Kim K, Park H, Lim K-M. Phototoxicity: Its Mechanism and Animal Alternative Test Methods. *Toxicological Research*. 2015;31(2):97-104.
25. Brem R, Guven M, Karran P. Oxidatively-generated damage to DNA and proteins mediated by photosensitized UVA. *Free radical biology & medicine*. 2017;107:101-9.
26. Schnellmann RG. Casarett and doull's toxicology the basic science of poisons. In: Klaassen CD, editor.2007.
27. Frances C. Smoker's wrinkles: epidemiological and pathogenic considerations. *Clinics in dermatology*. 1998;16(5):565-70.
28. Halliwell B. Reactive species and antioxidants. Redox biology is a fundamental theme of aerobic life. *Plant Physiol*. 2006;141(2):312-22.
29. Dudonne S, Poupard P, Coutiere P, Woillez M, Richard T, Merillon JM, et al. Phenolic composition and antioxidant properties of poplar bud (*Populus nigra*) extract: individual antioxidant contribution of phenolics and transcriptional effect on skin aging. *Journal of agricultural and food chemistry*. 2011;59(9):4527-36.

30. Morry J, Ngamcherdtrakul W, Yantasee W. Oxidative stress in cancer and fibrosis: Opportunity for therapeutic intervention with antioxidant compounds, enzymes, and nanoparticles. *Redox biology*. 2016;11:240-53.
31. Ben Khedir S, Moalla D, Jardak N, Mzid M, Sahnoun Z, Rebai T. Pistacia lentiscus fruit oil reduces oxidative stress in human skin explants caused by hydrogen peroxide. *Biotech Histochem*. 2016;91(7):480-91.
32. Almeida IFMd. Desenvolvimento de um sistema semi-sólido contendo fitocompostos captadores de espécies reactivas Faculdade de Farmácia da Universidade do Porto; 2009.
33. Bouayed J, Bohn T. Exogenous antioxidants--Double-edged swords in cellular redox state: Health beneficial effects at physiologic doses versus deleterious effects at high doses. *Oxid Med Cell Longev*. 2010;3(4):228-37.
34. Henry B, Foti C, Alsante K. Can light absorption and photostability data be used to assess the photosafety risks in patients for a new drug molecule? *J Photochem Photobiol B*. 2009;96(1):57-62.
35. Onoue S, Suzuki G, Kato M, Hirota M, Nishida H, Kitagaki M, et al. Non-animal photosafety assessment approaches for cosmetics based on the photochemical and photobiochemical properties. *Toxicol In Vitro*. 2013;27(8):2316-24.
36. Onoue S, Hosoi K, Toda T, Takagi H, Osaki N, Matsumoto Y, et al. Intra-/inter-laboratory validation study on reactive oxygen species assay for chemical photosafety evaluation using two different solar simulators. *Toxicol In Vitro*. 2014;28(4):515-23.
37. Svobodova A, Zdarilova A, Vostalova J. Lonicera caerulea and Vaccinium myrtillus fruit polyphenols protect HaCaT keratinocytes against UVB-induced phototoxic stress and DNA damage. *J Dermatol Sci*. 2009;56(3):196-204.
38. Onoue S, Tsuda Y. Analytical studies on the prediction of photosensitive/phototoxic potential of pharmaceutical substances. *Pharmaceutical research*. 2006;23(1):156-64.
39. Gould JW, Mercurio MG, Elmetts CA. Cutaneous photosensitivity diseases induced by exogenous agents. *J Am Acad Dermatol*. 1995;33(4):551-73; quiz 74-6.
40. Watson M, Holman DM, Maguire-Eisen M. Ultraviolet Radiation Exposure and Its Impact on Skin Cancer Risk. *Semin Oncol Nurs*. 2016;32(3):241-54.
41. Onoue S, Kawamura K, Igarashi N, Zhou Y, Fujikawa M, Yamada H, et al. Reactive oxygen species assay-based risk assessment of drug-induced phototoxicity: classification criteria and application to drug candidates. *J Pharm Biomed Anal*. 2008;47(4-5):967-72.

42. Kleinman MH, Smith MD, Kurali E, Kleinpeter S, Jiang K, Zhang Y, et al. An evaluation of chemical photoreactivity and the relationship to phototoxicity. *Regul Toxicol Pharmacol.* 2010;58(2):224-32.
43. Kochevar IE. Phototoxicity Mechanisms: Chlorpromazine Photosensitized Damage to DNA and Cell Membranes. *Journal of Investigative Dermatology.* 1981;77(1):59-64.
44. Baumler W, Regensburger J, Knak A, Felgentrager A, Maisch T. UVA and endogenous photosensitizers--the detection of singlet oxygen by its luminescence. *Photochem Photobiol Sci.* 2012;11(1):107-17.
45. Lee YS, Yi JS, Lim HR, Kim TS, Ahn IY, Ko K, et al. Phototoxicity Evaluation of Pharmaceutical Substances with a Reactive Oxygen Species Assay Using Ultraviolet A. *Toxicol Res.* 2017;33(1):43-8.
46. Kienapfel A. A review of the advancements in photosafety testing with regard to ICH's new topic S10: Photosafety evaluation of pharmaceuticals: University of Bonn 2013.
47. S10 Photosafety Evaluation of Pharmaceuticals Guidance for Industry. January, 2015.
48. Ceridono M, Tellner P, Bauer D, Barroso J, Alepee N, Corvi R, et al. The 3T3 neutral red uptake phototoxicity test: practical experience and implications for phototoxicity testing--the report of an ECVAM-EFPIA workshop. *Regul Toxicol Pharmacol.* 2012;63(3):480-8.
49. Lynch AM, Wilcox P. Review of the performance of the 3T3 NRU in vitro phototoxicity assay in the pharmaceutical industry. *Exp Toxicol Pathol.* 2011;63(3):209-14.
50. OECD Guideline for testing of chemicals, In vitro 3T3 NRU phototoxicity test, 432. 13 April 2004.
51. Spielmann H, Muller L, Auerbeck D, Balls M, Brendler-Schwaab S, Castell JV, et al. The second ECVAM workshop on phototoxicity testing. The report and recommendations of ECVAM workshop 42. *Altern Lab Anim.* 2000;28(6):777-814.
52. REACTIVE OXYGEN SPECIES (ROS) ASSAY TO EXAMINE PHOTOREACTIVITY OF CHEMICALS. ROS assay Validation Management Team; 2013.
53. Baccarin T, Mitjans M, Lemos-Senna E, Vinardell MP. Protection against oxidative damage in human erythrocytes and preliminary photosafety assessment of Punica granatum seed oil nanoemulsions entrapping polyphenol-rich ethyl acetate fraction. *Toxicol In Vitro.* 2015;30(1 Pt B):421-8.

54. Tang Y, Nakashima S, Saiki S, Myoi Y, Abe N, Kuwazuru S, et al. 3,4-Dihydroxyphenylacetic acid is a predominant biologically-active catabolite of quercetin glycosides. *Food Res Int*. 2016;89(Pt 1):716-23.
55. Kakkar S, Bais S. A review on protocatechuic Acid and its pharmacological potential. *ISRN Pharmacol*. 2014;2014:952943.
56. Semaming Y, Pannengetch P, Chattipakorn SC, Chattipakorn N. Pharmacological properties of protocatechuic Acid and its potential roles as complementary medicine. *Evid Based Complement Alternat Med*. 2015;2015:593902.
57. SpecialChem. Cosmetic Ingredients [Available from: <https://cosmetics.specialchem.com/>]. [28 september 2018].
58. Seok JK, Boo YC. p-Coumaric Acid Attenuates UVB-Induced Release of Stratifin from Keratinocytes and Indirectly Regulates Matrix Metalloproteinase 1 Release from Fibroblasts. *Korean J Physiol Pharmacol*. 2015;19(3):241-7.
59. Zang LY, Cosma G, Gardner H, Shi X, Castranova V, Vallyathan V. Effect of antioxidant protection by p-coumaric acid on low-density lipoprotein cholesterol oxidation. *Am J Physiol Cell Physiol*. 2000;279(4):C954-60.
60. Kot B, Wicha J, Piechota M, Wolska K, Grużewska A. Antibiofilm activity of trans-cinnamaldehyde, p-coumaric, and ferulic acids on uropathogenic *Escherichia coli*. *Turkish Journal of Medical Sciences*. 2015;45:919-24.
61. Yang J, Guo J, Yuan J. In vitro antioxidant properties of rutin. *LWT - Food Science and Technology*. 2008;41(6):1060-6.
62. Pyo S, Meinke M, Keck C, Müller R. Rutin—Increased Antioxidant Activity and Skin Penetration by Nanocrystal Technology (smartCrystals). *Cosmetics*. 2016;3(1):9.
63. Kumar N, Pruthi V. Potential applications of ferulic acid from natural sources. *Biotechnol Rep (Amst)*. 2014;4:86-93.
64. Rivelli DP, Filho CA, Almeida RL, Ropke CD, Sawada TC, Barros SB. Chlorogenic acid UVA-UVB photostability. *Photochemistry and photobiology*. 2010;86(5):1005-7.
65. Xiang Z, Ning Z. Scavenging and antioxidant properties of compound derived from chlorogenic acid in South-China honeysuckle. *LWT - Food Science and Technology*. 2008;41(7):1189-203.
66. Baek B, Lee SH, Kim K, Lim HW, Lim CJ. Ellagic acid plays a protective role against UV-B-induced oxidative stress by up-regulating antioxidant components in human dermal fibroblasts. *Korean J Physiol Pharmacol*. 2016;20(3):269-77.
67. Ortiz-Ruiz CV, Berna J, Tudela J, Varon R, Garcia-Canovas F. Action of ellagic acid on the melanin biosynthesis pathway. *J Dermatol Sci*. 2016;82(2):115-22.

68. Saija A, Tomaino A, Cascio RL, Trombetta D, Proteggente A, De Pasquale A, et al. Ferulic and caffeic acids as potential protective agents against photooxidative skin damage. *Journal of the Science of Food and Agriculture*. 1999;79(3):476-80.
69. Magnani C, Isaac VLB, Correa MA, Salgado HRN. Caffeic acid: a review of its potential use in medications and cosmetics. *Anal Methods*. 2014;6(10):3203-10.
70. Kyung Dong Kim MHS, Eul Kgun Yum,, Ok Seon Jeon, Young Woon Ju, Chang aMS. 2,4-Dihydroxycinnamic Esters as Skin Depigmenting Agents. *Bull Korean Chem Soc*. 2009;30(7).
71. Rekus MT. Characterization of growth and differentiation of a spontaneously immortalized keratinocyte cell line (HaCat) in a defined, serum-free culture system 2000.
72. Spikes JD. Photosensitizing properties of quinine and synthetic antimalarials. *Journal of Photochemistry and Photobiology B: Biology*. 1998;42(1):1-11.
73. Pluemsamran T, Onkoksoong T, Panich U. Caffeic acid and ferulic acid inhibit UVA-induced matrix metalloproteinase-1 through regulation of antioxidant defense system in keratinocyte HaCaT cells. *Photochemistry and photobiology*. 2012;88(4):961-8.
74. Cha JW, Piao MJ, Kim KC, Yao CW, Zheng J, Kim SM, et al. The Polyphenol Chlorogenic Acid Attenuates UVB-mediated Oxidative Stress in Human HaCaT Keratinocytes. *Biomol Ther (Seoul)*. 2014;22(2):136-42.